2010

Modulation of APP Processing and Amyloid-P Levels by Human 82-kDa Choline Acetyltransferase

Fatima S. Abji
Western University

Modulation of APP Processing and Amyloid-β Levels by Human 82-kDa Choline Acetyltransferase

(Spine title: Effects of Choline Acetyltransferase on Amyloid Production)

(Thesis format: Monograph)

By

Fatima S. Abji

Graduate Program in Physiology

Submitted in partial fulfillment
Of the requirements for the degree of
Master of Science

School of Graduate and Postdoctoral Studies
The University of Western Ontario
London, Ontario, Canada

THE UNIVERSITY OF WESTERN ONTARIO
SCHOOL OF GRADUATE AND POSTDOCTORAL STUDIES

CERTIFICATE OF EXAMINATION

Supervisor	Examiners
Dr. Jane Rylett	Dr. Vania Prado
Supervisory Committee	Dr. Dan Hardy
Dr. Marco Prado	Dr. Susan Meakin
Dr. Frank Beier	

The thesis by

Fatima Salima Abji

entitled:

Modulation of APP Processing and Amyloid-β Levels by Human 82-kDa Choline Acetyltransferase

is accepted in partial fulfillment of the
requirements for the degree of
Master of Science

Date_____ _____
Chair of the Thesis Examination Board

ABSTRACT

The 82-kDa isoform of choline acetyltransferase (82-ChAT) is unique to primates and is found in cholinergic cell nuclei. The functional significance of this protein is not well understood. Previous studies showed that nuclear 82-ChAT levels decrease with advancing age, and this is accelerated in Alzheimer's disease (AD). The present studies examined the effect of 82-ChAT on amyloid precursor protein (APP) metabolism and amyloid-β (Aβ) production. Levels of enzymes involved in processing of APP were examined in human SH-SY5Y neuroblastoma cells and in primary neuronal cultures prepared from cerebral cortex of embryonic APP/PS1 double transgenic mice that serve as a model of AD. A significant amount of $A\beta_{1-42}$ was released into cell culture media from neurons cultured from transgenic mice for 8 DIV, and this was associated with an elevation of total APP levels rather than changes in levels of APP processing enzymes. Upon expression of 82-ChAT, a 20% reduction in $A\beta_{1-42}$ release was found when compared to GFP-expressing control neurons. This was associated with a significant reduction in the protein but not mRNA of the β-secretase BACE1, indicating that 82-ChAT may alter proteins involved in post-translational modification and regulation of BACE1. These studies have important implications for AD pathology and broaden our understanding of the function of 82-ChAT proteins.

Keywords: choline acetyltransferase, cholinergic, Alzheimer's disease, amyloid-β, secretases, amyloid precursor protein, presenilin 1

CO-AUTHORSHIP

Studies described in this thesis were performed by Fatima S. Abji, with the following assistance:

(1) Ewa Jaworski assisted with immunocytochemistry experiments for Aβ in primary neuron cultures and 82-ChAT in SH-SY5Y cells and primary neuron cultures.

(2) Ewa Jaworski and Elizabeth Banasikowska assisted in the engineering of the 82-ChAT-SY5Y stable transformants.

(3) Ewa Jaworski assisted in breeding of mice and preparation of primary neuron cultures.

(4) Daisy Wong assisted in conducting ChAT activity assays.

(5) Dr. Rob Gros and Qingming Ding assisted in generation of 82-ChAT adenovirus.

(6) GFP adenovirus was a gift from the laboratory of Dr. Sean Cregan.

All experiments were carried out by Fatima S. Abji in the laboratory of Dr. R.J. Rylett. The thesis was written by Fatima S. Abji.

To Mom, Dad, Ali, Charles and Nina –
Thanks for your continuous support and prayers.

ACKNOWLEDGEMENTS

I would like to thank my supervisor, Dr. R.J. Rylett for her continued encouragement and guidance. You were always supportive and understanding at every step of this process. I have also found much help and support in the Rylett lab over these past two years, and am thankful to Elizabeth Banasikowska, Alexis Gordon, Kirk Young, Ventzi Hristova, Kathi James, Stefanie Black, Daisy Wong, Rachel Mixer, Leah Cuddy, and Sebastian Borosciwz. Special thanks to Ewa Jaworski, who was always patient and accommodating.

I would also like to thank the members of my advisory committee, Dr. Frank Beier and Dr. Marco Prado for their helpful advice and guidance. Finally, I would like to thank my family and friends for their unconditional love and support.

TABLE OF CONTENTS

LIST OF TABLES

LIST OF FIGURES

LIST OF APPENDICES

LIST OF ABBREVIATIONS

^{11}C-PIB	^{11}C labelled Pittsburgh compound B
Aβ	Amyloid-β
Acetyl CoA	Acetyl coenzyme A
ACh	Acetylcholine
AChE	Acetylcholinesterase
AChRs	Acetycholine receptors
AD	Alzheimer's disease
ADAM10	A disintegrin and metalloproteinase 10
AICD	Amyloid precursor protein intracellular domain
APOE ε4	Apolipoprotein E ε4 allele
APP	Amyloid precursor protein
BACE1	β-site APP cleaving enzyme 1
BuChE	Butyrylcholinesterase
c83	Carboxy-terminal fragment 83
c99	Carboxy-terminal fragment 99
CAA	Cerebral amyloid angiopathy
CDK5	Cyclin dependent kinase 5
CDR	Clinical Dementia Rating
ChAT	Choline acetyltransferase
CHT	Choline transporter
CNS	Central nervous system
CSF	Cerebrospinal fluid

DIV	Days *in vitro*
DMEM	Dulbecco's modified Eagle medium
E14-17	Embryonic day 14-17
ECL	Enhanced ChemiLuminescence
EOFAD	Early-onset form of Alzheimer's disease
ER	Endoplasmic reticulum
FBS	Fetal bovine serum
G-418	Genticin
GAPDH	Glyceraldehyde-3-phosphate dehydrogenase
GSK3β	Glycogen synthase kinase 3β
HEK 293	Human embryonic kidney cells
ifu	Infectious units
KPI	Kunitz protease inhibitor
MCI	Mild Cognitive Impairment
MEM	Minimum Essential Medium
MMSE	Mini-Mental State Examination
MOI	Multiplicity of infection
MRI	Magnetic resonance imaging
NBM	Nucleus basalis of Meynert
NeuN	Neuronal nuclear protein
NFTs	Neurofibrillary tangles
NGF	Nerve growth factor
NGFr	Nerve growth factor receptor

NLS	Nuclear localization signal
NPCs	Nuclear pore complexes
NRSE	Neuron-restrictive silencer element
NTC	No template control
NTG	Non-transgenic
PBS	Phosphate buffer saline
PET	Positron emission tomography
PKC	Protein kinase C
PNS	Peripheral nervous system
PS1	Presenilin 1
PS2	Presenilin 2
sAPPα	Soluble APPα
sAPPβ	Soluble APPβ
SEM	Standard error of the mean
TG	Transgenic
TGN	Trans-Golgi-network
VCP	Valosin-containing protein
VAChT	Vesicular ACh transporter

CHAPTER ONE: GENERAL REVIEW OF LITERATURE

Alzheimer's disease (AD) is a neurodegenerative disorder that is a leading cause of cognitive disability and morbidity in the elderly in North America today. According to a report released by the Alzheimer Society of Canada in 2010, half of a million Canadians have AD or related dementia. Currently one person develops AD every 5 minutes and this will reach one person every 2 minutes by the year 2038. These overwhelming statistics highlight the importance of understanding AD etiology in order to develop effective treatments and preventions in the near future.

The cholinergic system, which includes neurons or synapses that produce and release the neurotransmitter acetylcholine (ACh), is the major neuronal system affected in brains of individuals with AD. Choline acetyltransferase (ChAT), the enzyme responsible for the synthesis of ACh, serves as a phenotypic marker of cholinergic neurons because of its selective expression in these cells. A decline in ChAT activity is found in selected regions of necropsy brain of individuals with AD and is associated with degeneration of these neurons. The deficits in ChAT activity are also positively correlated with the cognitive impairments observed in AD. The studies undertaken in this thesis were aimed at expanding our current knowledge of the function of ChAT proteins, particularly in relation to aspects of AD pathology such as amyloid protein metabolism.

1.1 Alzheimer's disease

1.1.1 General features

The majority of AD cases are sporadic, with age being the largest risk factor for developing the disease. A small percentage of AD cases are inherited in an autosomal dominant manner related to mutations in the amyloid precursor protein (APP), presenilin 1 (PS1) and presenilin 2 (PS2) (Goate et al 1991; Rogaev et al 1995). This early-onset form of AD (EOFAD) accounts for less than 10 percent of total individuals affected and is clinically indistinguishable from AD. Additionally, kindreds with EOFAD with no identifiable mutations in these genes have been documented and in these cases the disease may be caused by other mutations that have not yet been characterized. Inheritance of the ε4 allele of apoplipoprotein E (APOE ε4) doubles the risk of AD whereas the absence of APOE ε4 decreases the risk by 40% (Seshadri et al 1995). The mechanisms by which the different APOE alleles alter AD age of onset and risk are unknown and are the subject of current research.

The majority of AD cases are late-onset, with individuals generally diagnosed with dementia after the age of 65 years. However, the earliest changes can occur 20 years before the appearance of clinical symptoms. On average, individuals often live 8-10 years after receiving a diagnosis of AD, but some individuals may live with the disease for up to 20 years. Although the course of the disease can vary significantly between individuals, there are trends in the progression of symptoms. Mild AD (also known as mild cognitive impairment, MCI) generally lasts from 2 to 4 years. In this stage, individuals

experience mild memory loss, and are slow to learn new things. One of earliest features of this stage is a decline in episodic memory, the long-term memories of autobiographical events (Bondi et al 1995, 1999). Moderate AD is the longest stage and generally lasts from 2 to 10 years. In this stage, individuals become disabled as they become more disoriented and forget recent events and have trouble recognizing familiar individuals. They also have difficulty communicating and develop speech problems. Severe AD, which often lasts from 1 to 5 years, involves complete loss of control of bodily functions and requires constant care. Individuals generally have almost non-existent memory and cannot recognize people or speak. They become highly susceptible to other illnesses such as respiratory or other infections due to their weakened state.

1.1.2 Pathological characteristics

The formation of amyloid-β (Aβ) plaques and neurofibrillary tangles (NFTs) are considered to be the pathological hallmarks of AD (Braak and Braak 1991). NFTs are intracellular lesions formed from hyperphosphorylation of tau, a protein that is involved in microtubule stability. The microtubule-binding domain of tau interacts with the β-tubulin proteins found at inner surfaces of microtubules and the positively charged proline-rich region of tau interacts with the negatively charged microtubule surface (Kar et al 2003; Amos 2004). This promotes the polymerized state of microtubules which enables the proper transport of cargo within cells and maintains the strength of the cytoskeleton. The binding affinity of tau to microtubules is regulated post-translationally primarily by serine/threonine-

directed phosphorylation (Mazanetz and Fischer 2007). In AD, the balance between phosphorylation and dephosphorylation of tau is disrupted, and a greater proportion of tau is found in the cytoplasm where it becomes susceptible to aggregation (Ballatore et al 2007).

Aβ is produced as a peptide comprised of between 39 and 43 amino acids from proteolysis of APP. As shown in Figure 1.1, cleavage of APP by the β-secretase releases sAPPβ and gives rise to a c99 fragment which is then processed by the γ-secretase complex to produce $A\beta_{1-40}$ or $A\beta_{1-42}$ and the amino-terminal APP intracellular domain (AICD). β-site APP cleaving enzyme 1 (BACE1) is the major β-secretase in the brain (Vassar et al 1999). Physiological roles for this amyloidogenic processing pathway are beginning to be elucidated. For example, β-secretase cleavage of APP has been implicated to play a role in normal apoptosis during development. The amino-terminal fragment of APP is a ligand for death receptor 6, activating a self-destruction pathway important for normal sculpting of axons (Nikolaev et al 2009). Aβ production is precluded in the non-amyloidogenic pathway where APP is cleaved by an α-secretase which releases sAPPα and a c83 fragment that is processed by the γ-secretase complex to generate p3 and AICD. α-secretase activity is mediated by one or more zinc metalloproteinases such as ADAM10 or ADAM9 (Thinkaran and Koo 2008).

The exact location for Aβ production is still a topic of debate. APP is initially synthesized in the endoplasmic reticulum (ER) and transported through the trans-Golgi-network (TGN) where the majority of APP resides at a steady

state (Xu et al 1997; Greenfield et al 1999). APP is transported to the cell surface in TGN-derived secretory vesicles, where the majority of α-secretase cleavage occurs (Sisodia 1992). Only about 10 percent of total APP molecules are found at the cell surface. Re-internalization of APP to the endosomal/lysosomal degradation pathway occurs rapidly due to a strong YENPTY endocytosis motif located near the carboxyl terminus. BACE1 activity is thought to be a rate-limiting factor for Aβ generation, and requires an acidic environment for optimal function. The major cellular compartments where BACE1 activity has been observed include the early Golgi, late Golgi/early endosomes, endosomes, and the cell surface (Vassar et al 1999; Walter et al 2001; Huse et al 2000, 2002). Mechanisms regulating BACE1 trafficking and activity are not fully understood and remain a focus of current research.

Aβ peptides accumulate as oligomeric and then fibrillar aggregates which then form into extracellular plaques of AD. $A\beta_{1-40}$ is the most common Aβ species found, whereas $A\beta_{1-42}$ has a greater tendency towards aggregation due to the additional two hydrophobic residues at the carboxyl terminus. It is considered that Aβ is not toxic as monomers but aggregated forms of the peptide, especially oligomers, are toxic to neurons and can alter synaptic transmission (Noguchi et al 2009).

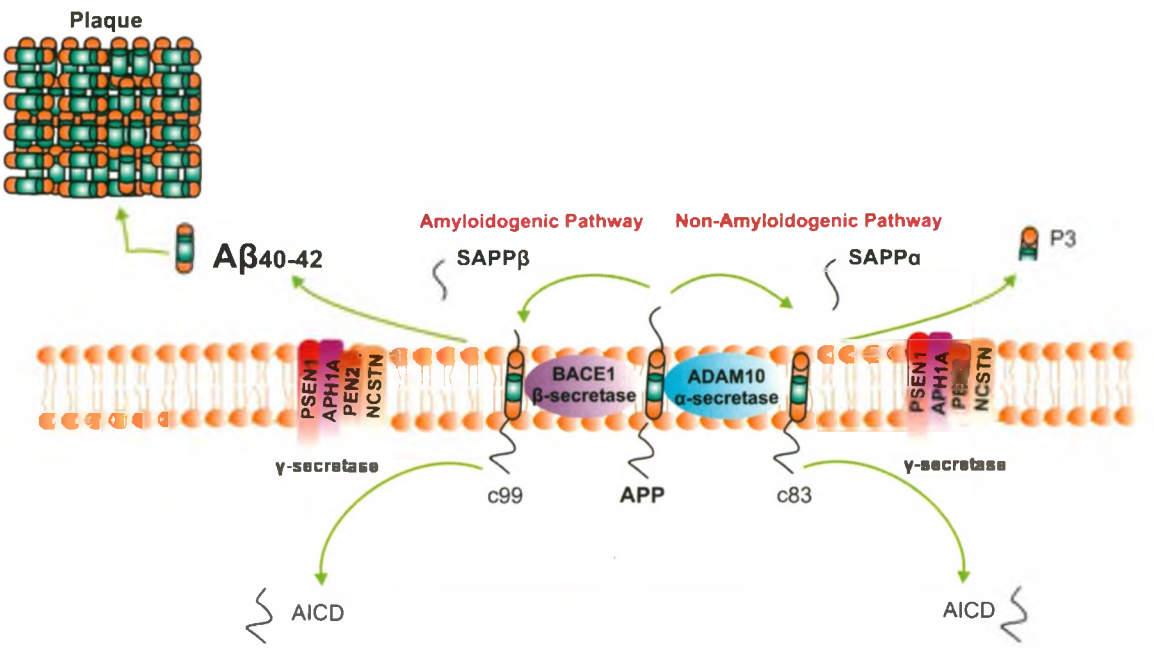

Figure 1.1: Proteolytic processing pathways of APP. Cleavage of APP along the amyloidgenic pathway involves processing by a β secretase (BACE1) and γ secretase complex. This results in production of either a 40 or 42 residue Aβ peptides that can aggregate into the extracellular plaque deposits observed in AD. Alternatively, Aβ production is precluded by cleavage within the Aβ domain by an α secretase (ADAM10) along the non-amyloidogenic pathway.

The other major pathological feature of AD is neurodegeneration, with the hippocampus and cortex, including the frontal, temporal and parietal lobes being the major brain areas affected. The hippocampus is a component of the limbic system that is affected early in AD. This system is involved with memory and emotion, and is primarily associated with processing of verbal and visual memory. It also joins the two hemispheres of the brain connecting emotion and memory with behaviour. The entorhinal cortex, found in the medial temporal lobe, is the region where atrophy is first visible in the AD brain (Feldman et al 2008). The temporal lobes are important for control of new learning and short-term memory. The frontal lobe is involved in motor control and some cognitive processes while the parietal lobes allow us to put activities in sequence and understand spatial information. These neocortical areas deteriorate as the disease progresses (Braak and Braak 1991).

Cholinergic neurons are the major sites of neurodegeneration in AD, with cholinergic neurons that have their cell bodies in basal forebrain nuclei being the primary source affected. This includes neurons that project from the nucleus basalis of Meynert (NBM) to areas of the cortex (frontal, parietal and occipital cortices), as well as those that project from the diagonal band of Brocca through the medial septum to the hippocampus (Davies and Maloney 1976; Fibiger 1982; Mesulam 1996). Other neuron types are also affected in AD, including the serotonergic cells of the dorsal raphe (Michelsen et al 2008), dopaminergic neurons of the substantia nigra (Zarow et al 2009) and noradrenergic neurons of the locus coeruleus (Zarow et al 2003; Heneka et al 2010).

1.1.3 Diagnosis

The only definitive diagnosis for AD can be made at post-mortem. In the clinical setting, AD is confirmed by elimination of other diseases through evaluation of patient medical history, neuropsychological testing and interviews with family members (Feldman et al 2008). The most widely used test to distinguish dementia from normal cognitive decline due to aging is the Mini-Mental State Examination (MMSE) (Folstein et al 1975). The severity of disease is determined with the Clinical Dementia Rating (CDR) scale, where 0 denotes no cognitive impairment, 0.5 is very mild dementia, 1 is mild dementia, 2 is moderate dementia and 3 is severe dementia. Patients are assessed in six areas of cognitive and functional performance: memory, orientation, judgment and problem solving, community affairs, home and hobbies, and personal care (Morris 1993, 1997). When available, magnetic resonance imaging (MRI) scans are also used as diagnostic tools. Structural imaging is used to look for degeneration of vulnerable areas such as the hippocampus and entorhinal cortex and can be used to predict the progression from MCI to AD. Also, these images allow physicians to rule out other pathologies such as tumours or non-AD degeneration (Feldman et al 2008).

Positron Emission Tomography (PET) using radiological markers has brought new possibilities for early diagnostic tools for AD. One example is the carbon-11 (^{11}C) labelled Pittsburgh compound B (^{11}C-PIB), which is a ^{11}C derivative of the thioflavin-T dye that is used to stain neuritic Aβ plaques (Rowe et al 2007). Studies have shown an approximately 2-fold increase in binding of

^{11}C-PIB to plaques in AD cases compared to control subjects, and may be used to indicate disease progression (Rowe et al 2007; Klunk et al 2004).

Currently, no definite biomarkers have been established that distinguish individuals with AD from normally aging subjects. Cerebrospinal fluid (CSF) levels of $A\beta_{1-42}$ (Iwatsubo 1998), total tau (Sunderland et al 2003) and phospho-tau (Vanmechelen et al 2000) are the most reproducible indicators of EOFAD. A decrease in CSF $A\beta_{1-42}$ and increase in phospho-tau levels have been shown to correlate with EOFAD (Sunderland et al 2003) and may also predict the conversion of MCI to AD (Riemenschneider et al 2002).

1.1.4 Treatment

There are four drugs currently approved by Health Canada that act to reduce symptoms of AD. Three of these, donepezil, galantamine, and rivastigmine, are acetylcholinesterase (AChE) inhibitors, and the other is memantine, an NMDA receptor antagonist. AChE inhibitors act by decreasing the breakdown of ACh thus counteracting the effect of degenerating cholinergic neurons and the decrease in ACh release. These pharmacological tools are most commonly used for mild to moderate cases of AD (Ritchie et al 2004; Rockwood 2004). Memantine acts by targeting NMDA receptors that are concentrated in the hippocampus and cortex. Excess glutamate, termed excitotoxicity, binds to NMDA receptors to cause over-activation and resulting in apoptosis of neurons in the brain (Sucher et al 1997). In AD, Aβ plaques make neurons more susceptible to the effects of excitotoxicity (Koh et al 1990). Memantine acts as a fast-binding

antagonist, binding to spots on activated NMDA receptors thus preventing glutamate-induced over-activation (Chen and Lipton 1997). Memantine can be beneficial in moderate to advanced AD cases by improving global cognition parameters (Winblad and Poritis 1999); improvements in behavioural parameters in AD patients has only been shown when memantine is combined with donepezil (Tariot et al 2004).

Recently, anti-Aβ immunization therapies have been under development. Both active and passive immunization strategies have produced positive results in animal models, but limited success has been seen in human clinical trials. Initial Aβ immunotherapy studies in animal models reduced Aβ load and restored cognitive defects (Schenk et al 1999). The first phase I clinical trial for active immunization in humans in 2000, did not reveal adverse side effects and patients formed antibodies against $A\beta_{1-42}$. However, larger phase IIa clinical trials were terminated early because some patients developed subacute encephalopathy due to meningoencephalitis (Orgogozo et al 2003). Although these initial trials did yield some success in developing antibodies against $A\beta_{1-42}$ and reducing plaque load, there is controversy regarding the ability of immunotherapy to slow disease progression and improve cognitive parameters (Gilman et al 2005).

1.1.5 Etiology

The exact mechanisms that lead to the formation of Aβ plaques and NFTs, and to neuron cell loss are unknown and remain the focus of a large research effort. Several hypotheses have been advanced about the etiology of AD. The

cholinergic hypothesis was formulated based on the fact that cholinergic deficits are consistently observed in AD (Whitehouse 1981; Rylett et al 1983; Nilsson et al 1986; Aubert et al 1992; Davis et al 1999), as well as the finding that blockade of brain cholinergic neurotransmission negatively impacts cognitive function in neurologically-normal individuals (Drachman and Sahakian 1980). In this hypothesis, the cognitive decline found in AD is due to a decrease in cholinergic neurotransmission. The major pharmacological tool available for treatment of AD is the AChE inhibitors, which potentiate cholinergic transmission. However, these drugs are only effective in reducing symptoms in a small proportion of AD subjects (Rogers et al 1998; Gauthier 2002).

The amyloid hypothesis is centered on Aβ deposition as the underlying cause of the cognitive decline of AD (Hardy and Selkoe 2002). This is supported by the fact that mutations in APP, PS1 and PS2 that are associated with EOFAD lead to increased Aβ production that favours the toxic $A\beta_{1-42}$ form of the protein (Citron et al 1992; Jankowsky et al 2004). Also, individuals with Down's Syndrome, or trisomy 21, have an extra copy of the APP gene and are prone to developing AD as early as the fourth decade of life (Rumble et al. 1989). Aβ accumulation may occur 10-15 years prior to signs of dementia emerging and peak during mild AD with little increase afterwards. Individuals with MCI have abundant senile plaques throughout the neocortex and NFTs in the hippocampus and entorhinal cortex (Price and Morris 1999). Continued exposure to high concentrations of Aβ at a pre-clinical stage of AD may be important in driving cell loss and cognitive decline.

It has also been postulated in recent years that Aβ plaques and NFTs are the result of an attempt by vulnerable neurons to re-enter the cell cycle. Traditionally, neurons are considered to be terminally differentiated cells and hence should remain in G_o phase of the cell cycle. In AD, dysregulation of the cell cycle and re-expression of cell cycle markers occurs early in disease pathogenesis, before the formation of Aβ plaques and NFTs (Yang et al 2006). These neurons are pushed through DNA replication (Yang et al 2001) and into the G_2 phase of the cell cycle where they are arrested for long periods of time. The result is a state that is permissive, but not sufficient, to induce cell death.

The activation of kinases, such as cyclin dependent kinase 5 (CDK5) and glycogen synthase kinase 3β (GSK3β), and the downregulation of phosphatases, such as protein phosphatase 2A and 2B, is a predominant feature of the G_2 phase of the cell cycle. This shift in balance towards phosphorylation leads to hyperphosphorylation of tau by protein kinases, CDK5 and GSK3β, resulting in NFT formation. Over-activation of CDK5 is also associated with increased Aβ production through phosphorylation of APP (Iijima et al 2000; Liu et al 2003) and increased activity of the β-secretase BACE1 (Cruz et al 2006; Wen et al 2008). These proteins further stimulate other neurons to re-enter the cell cycle and continue this cycle, eventually pushing neurons to the point of cell death (Yang et al 2001; Varvel et al 2008).

Other mechanisms implicated in AD include oxidative stress, excitotoxicity, and neuroinflammation. AD is a complex disorder that is probably the result of a combination of these mechanisms and insults. To develop effective treatments

and preventions for AD, it is important to understand the sequence of these events, and how they fit together to contribute to disease pathology and progression.

1.2 Genetically-modified mouse models of AD

Several mouse models have been developed in an attempt to replicate the pathological features and progression of AD. The development of transgenic technologies has allowed significant advances in models that recapitulate various AD-related pathologies. The mouse lines that have been best characterized are those that replicate amyloid pathology by introducing APP and PS1 that have mutations that are found in cases of EOFAD. Three isoforms of APP result from alternative splicing of a single gene product. APP_{695} is the most abundant of these and is expressed in neurons. The APP_{751} and APP_{770} isoforms are found in non-neuronal cells and contain a Kunitz-protease inhibitor domain that is not present in APP_{695} (Suzuki and Nakaya 2008). Mutant residues in APP are found within the Aβ domain, as well as flanking the amino and carboxyl termini. Figure 1.2 shows the sites of APP cleavage and the resulting Aβ peptide sequence. Various residues that are mutated in EOFAD cases and used for murine models of AD are highlighted. Transgenic animals that express a mutant PS1 alone do not develop significant Aβ deposits or AD-like pathology. However, when these mice are combined with APP mutant lines, the Aβ pathology is observed in younger animals and the ratio of $Aβ_{1-40}$:$Aβ_{1-42}$ shifts to favour $Aβ_{1-42}$ when compared to animals expressing mutant APP alone (Jankowsky et al 2004).

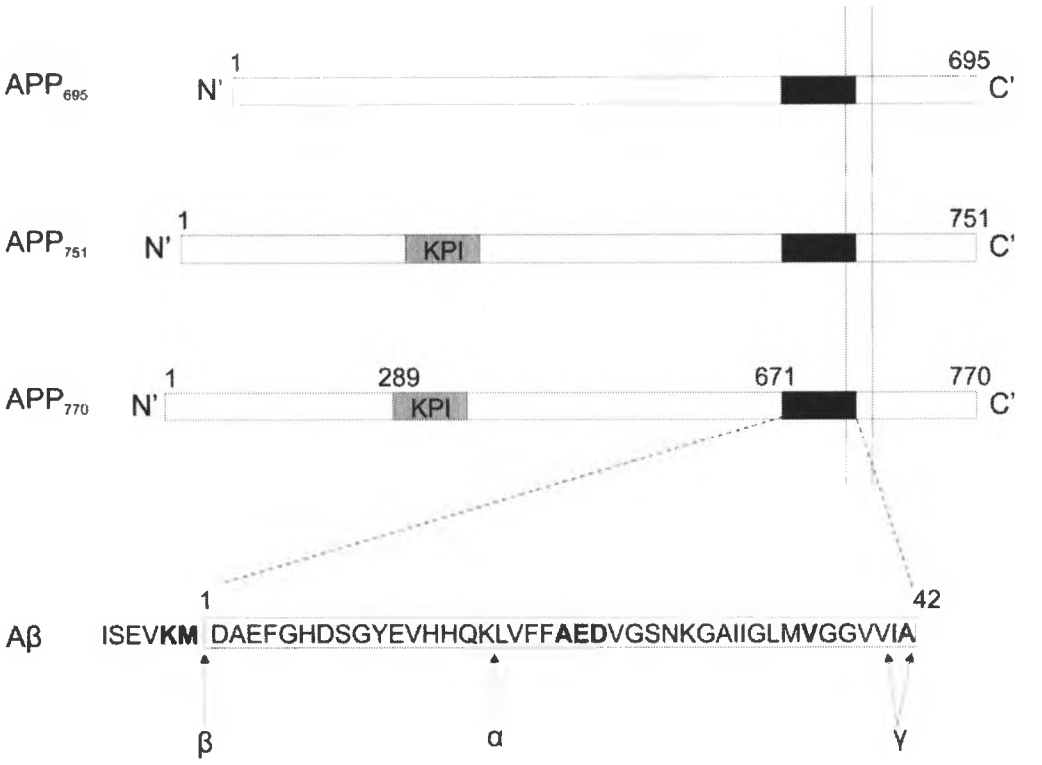

Figure 1.2: Schematic diagram of human APP. The three major isoforms of human APP in the brain are shown. APP_{770} and APP_{751} contain a Kunitz protease inhibitor (KPI) domain that is not present in APP_{695}.The black box indicates the region of APP that forms the Aβ peptide. The plasma membrane is represented by vertical black lines. The Aβ domain is enlarged and amino acid sequence is given. Sites of APP cleavage are indicated for each secretase (α, β, γ). Major residues associated with mutations in the early-onset form of AD are shown in bold. These include the Swedish (K670N/M671L), Flemish (A692G), Arctic (E693G), Italian (E693K), Dutch (E693Q), Iowa (D694N), Indiana (V717F), and London (V717I) mutations.

The first model to display significant AD-like pathology was the PDAPP mouse, expressing human APP with the Indiana mutation (V717F). In this model, significant dense core plaques and dystrophic neurites are found in the hippocampus and cortex beginning at 6-9 months of age (Games et al 1995). Since the development of this model in the late 1990s, several other murine models of AD pathology have been created with single or multiple EOFAD mutations. These models and the observations of AD-like pathology are summarized in Table 1.1.

The APP/PS1ΔE9 model has been well characterized for its extensive Aβ pathology. Plaques are found as early as 4 months of age and continue to increase until animals are 12 months old (Garcia-alloza et al 2006, Machova et al 2008). There are also significant changes in cholinergic neurons in this model. Dystrophic cholinergic (ChAT-positive) neurites are observed in the cortex and hippocampus by 2-3 months and in the striatum by 5-6 months that increase in parallel to Aβ deposition. Although the number of ChAT-positive neurons are not altered with age, a decrease in ChAT enzyme activity is observed in the cortex and hippocampus (Perez et al 2007). Age-related deficits observed in another cholinergic marker, AChE, correlate weakly with diminished performance on the repeated reversals task, a measurement of episodic-like memory. The majority of the cognitive decline observed in these animals is due to the extensive Aβ load (Savonenko et al 2005). The relatively early onset of Aβ production and the extensive plaque burden and resulting cholinergic deficits in these mice provides a powerful model for the study of the role of Aβ in AD pathology.

Table 1.1: Common murine models of Alzheimer's disease

Mouse Model	Mutations	Promoter	Age of Aβ Deposition	General Pathology	References
PDAPP	hAPP (all isoforms) with Indiana mutation (V717F)	PDGF-β	6-9 months	- At 6-9 months, human Aβ found in hippocampus, corpus callosum and cerebral cortex, increasing with age - Plaques range from diffuse irregular types to compacted plaques (thioflavin S positive) - Synaptic damage and neuroinflammation (astrocytosis, microgliosis) observed - Decreased staining for presynaptic (synaptophysin) and dendritic (MAP-2) markers - Reduction in ChAT positive nerve terminals in cortex and hippocampus prior to Aβ plaque formation - No differences in cholinergic cells in the basal forebrain with age	Games et al. 1995; German et al. 2003
Tg2576	$hAPP_{695}$ with Swedish mutation (K670N/ M671L)	Prion	Plaques by 9 months	- Dense plaques (thoiflavin S positive) found in cortex, subiculum, and presubiculum - GFAP-positive astrocytes associated with amyloid plaques - Evidence of dystrophic neurites but minimal cell death	Hsiao et al. 1996
APP/ PS1-A246E	$hAPP_{695}$ with Swedish mutation (K670N/ M671L) human PS1 (A246E)	Prion	Small deposits at 6 months; plaques at 9 months	- Aβ staining found in hippocampus and cortex as well as blood vessels in the leptomeninges and ascending vessels that travel into deep cortical layers - $Aβ_{-40}$:$Aβ_{1-42}$ is 1.75:1 - Plaques consist of hAβ core surrounded by mAβ while diffuse deposits are intermingled human and mouse Aβ - Females have higher amyloid burden	Van Groen et al. 2006; Jankowsky et al 2004

APP/ PS1ΔE9	$hAPP_{695}$ with Swedish mutation (K670N/ M671L) hPS1 (ΔE9)	Prion	Plaques by 4-6 months	- Aβ staining found in hippocampus and cortex - CAA observed in blood vessels in the leptomeninges beginning at 6 months of age - Large amount of deposits found in thalamus and cerebellum - $Aβ_{1-40}$:$Aβ_{-42}$ is 0.75:1 - Both insoluble and soluble Aβ levels increase with age, and insoluble $Aβ_{1-40}$:$Aβ_{1-42}$ shifts to favour $Aβ_{1-42}$ as measured by ELISA - Plaques consist of hAβ core surrounded by mAβ while diffuse deposits are intermingled human and mouse Aβ - Age related decline in activity of ChAT, AChE, BuChE - No significant change in ChAT-positive neurons in cortex, striatum, nucleus basalis except motor cortex	Van Groen et al. 2006; Jankowsky et al. 2004; Garcia-Alloza et al. 2006; Machova et al. 2008; Perez et al. 2007; Savonenko et al. 2005
3 X Tg-AD	$hAPP_{695}$ with Swedish mutation (K670N/ M671L) $hTau_{4R0N}$ (P301L) PS1 knock in (M146V)	Thy1	Intracellular deposits at 3-6 months; plaques from 6-12 months	- Intracellular Aβ initially found in neocortex (3-4 months) and then in hippocampus (6 months) - Plaques in frontal cortex (6 months) and then other cortical areas and hippocampus (12 months) - Reactive astrocytes colocalize with thioflavin S-positive Aβ deposits - Tau pathology begins in the pyramidal neurons of the hippocampus and progresses to cortex - Between 12 and 15 months, phospho-tau immunoreactivity is observed - Synaptic transmission is impaired by 6 months in the CA1 region of the hippocampus - E15-18 cortical cultures have increased Aβ levels (ELISA) and phospho-tau levels (immunoblotting) with increased time in culture	Oddo et al. 2003; Vale et al 2009

1.3 Components and anatomy of the cholinergic neuron systems

Cholinergic neurons synthesize the neurotransmitter acetylcholine (ACh) and are found throughout the central nervous system (CNS), autonomic pathways and peripheral nervous system (PNS). In the periphery, ACh is released at the neuromuscular junction and mediates voluntary muscle contraction (Oda 1999). In the CNS, ACh is released in areas involving learning, memory, sleep and arousal. The basal forebrain is the primary source of cholinergic neuronal perikarya that project to areas of the cortex and hippocampus (Fibiger 1982; Mesulam 1996).

There are 8 cholinergic neuron groups in the brain that are designated Ch1-Ch8 and defined based on the location of their perikarya. These regions project to other CNS structures and were identified initially in immunohisto-chemistry studies using polyclonal and monoclonal antibodies against ChAT (Eng et al 1974; Cozzari and Hartman 1980). These results were supported by studies that detected ChAT mRNA by *in situ* hybridization (Kasashima et al 1998). Ch1 neurons are located in the medial septal nucleus and Ch2 neurons are located in the vertical nucleus of the diagonal band of Brocca. Together, the Ch1 and Ch2 neurons project to the hippocampus. Ch3 neurons are found in the horizontal limb of the diagonal band nucleus and project to the olfactory bulb. The Ch4 neurons are associated with the NBM and innervate the cerebral cortex and amygdala. The basal forebrain contains these four regions which contain cholinergic cells. The proportion of cells in this area that are cholinergic varies from 1% in the Ch3 group to 90% in the Ch4 group (Mesulam 1995).

Ch5 and Ch6 neurons are associated with the pedunculopotine nucleus and laterodorsal tegmental nucleus in the rostral brainstem, respectively, and together they project to the thalamus. These regions likely also provide extrinsic projections to basal ganglia. One exception is the striatum which is largely comprised of intrinsic innervations from cholinergic interneurons (Fibiger 1982). In rodents, up to 30% of cholinergic innervation in the cortex may be accounted for by intrinsic interneurons; the existence of cholinergic interneurons in the primate cerebral cortex is still a topic of debate. Ch7 neurons are found in the medial habenula and project to the interpeduncular nucleus. Ch8 neurons lead from the parabigeminal nucleus to the superior colliculus (Mesulam 1988).

As shown in Figure 1.3, ACh is synthesized in cholinergic nerve terminals from acetyl coenzyme A (acetyl CoA) and choline by ChAT (Nachmansohn and Machado 1943). It is then transported into synaptic vesicles by the vesicular ACh transporter (VAChT) which relies on a proton electrochemical gradient generated by the H^+ pumping ATPase (Nguyen et al 1998). Upon neuronal depolarization, synaptic vesicle stores of ACh are recruited in a calcium-dependent manner (Richardson 1986) to active zones of the presynaptic nerve terminal (Collier and Katz 1974). Vesicles fuse to the plasma membrane and release ACh into the synaptic cleft where it binds to pre- and post-synaptic nicotinic or muscarinic receptors. Excess ACh in the synaptic cleft is degraded by AChE into choline and acetate. Choline is taken up into cholinergic presynaptic terminals primarily by the high-affinity sodium-dependent choline transporter (CHT) which is unique to cholinergic neurons (Kuhar and Murrin 1978; Okuda et al 2000) and is the rate-

limiting step for ACh synthesis. Choline is also taken up into all cells by a ubiquitous low-affinity sodium-independent transporter that is important for providing choline to cells for phosphatidylcholine synthesis (Kuhar and Murrin 1987; Lee et al 1993). CHT replenishes choline as substrate for synthesis of ACh reserves to maintain cholinergic neurotransmission.

As discussed previously, degeneration and dysfunction of cholinergic neurons is a major pathological feature of AD. This is associated with a decline in various markers of cholinergic neuron function, including ChAT activity (Perry et al 1977), high-affinity choline uptake (Rylett et al 1983), ACh release (Nilsson et al 1986) and ACh receptor (AChR) binding (Aubert et al 1992). Among these markers, a decrease in ChAT activity is found most consistently and correlates with a reduction in neurons of the NBM (Bird et al 1983; Henke and Lang 1983). ChAT activity in cortical areas is negatively correlated to the density of senile plaques and to cognitive impairment as determined by neuropsychological testing (Perry et al 1981; Mountjoy et al 1984). A better understanding of the cellular regulation and activity of ChAT is essential in discerning the vulnerability of the cholinergic system and how it is targeted in AD.

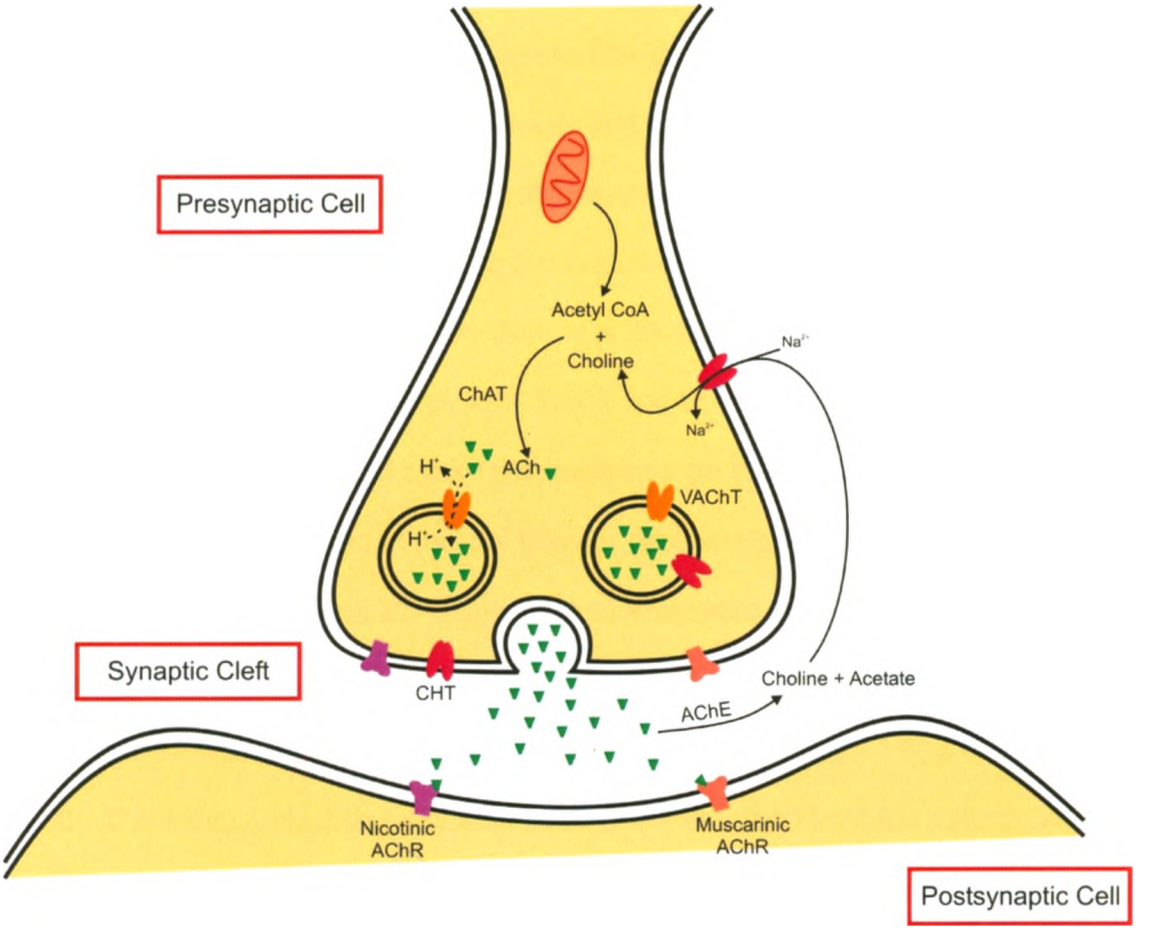

Figure 1.3: Cholinergic nerve terminal. In the presynaptic cell, acetylcholine (ACh) is synthesized by choline acetyltransferase (ChAT) from substrates acetyl CoA and choline. ACh is transported into synaptic vesicles by the vesicular acetylcholine transporter (VAChT) where it is stored. Upon depolarization, ACh is released into the synaptic cleft where it can bind to either nicotinic or muscarinic receptors on the pre- and post-synaptic cell. Excess ACh is degraded in the synaptic cleft by acetylcholinesterase (AChE) and choline can be taken up into the presynaptic cell primarily through the action of the high-affinity Na^{2+}-dependent choline transporter (CHT). This is the rate-limiting step for ACh synthesis.

1.4 Human 82-kDa choline acetyltransferase protein (82-ChAT)

Human ChAT contains two domains that consist of α-helices surrounding a six-stranded β-sheet. Binding of substrates choline and acetyl CoA occurs at residues 1 to 89 and 392 to 615, with the catalytic domain where ACh synthesis occurs involving residues 90 to 391 (Kim et al 2006). The active site histidine residue (H324) (Carbini and Hersh 1993) is found where the two domains meet in the middle of a water-filled tunnel that runs through the enzyme.

ChAT is synthesized in the cell body of cholinergic neurons with approximately 5-18% of rat ChAT molecules transported to nerve terminals by fast axoplasmic flow (30-200 mm/day) (Dziegielewska et al 1976) and the remainder transported by a slow flow rate (5-15 mm/day) (Wooten and Cheng 1980). The exact molecular mechanisms of ChAT transport from the neuron cell body to distal axonal terminals are still unknown. At the nerve terminal, the majority of ChAT (80-90% of total enzyme activity) is found in the cytoplasm and the remainder (10-20%) is bound non-ionically to the plasma membrane and/or synaptic vesicles (Schmidt and Rylett 1993; Pahud 1998).

ChAT is encoded by a single gene within the "cholinergic gene locus" located on chromosome 10 (Hahm et al 1997; Figure 1.4). This locus also contains the gene encoding VAChT as a single exon between R and N non-coding exons in the ChAT promoter. Multiple transcripts of ChAT are produced by alternative splicing and differential utilization of at least five non-coding exons (Misawa et al 1997). Seven mRNA isoforms of human ChAT have been identified: R1-, R2-, N1-, N2-, H-, S- and M-transcripts. All human ChAT mRNAs

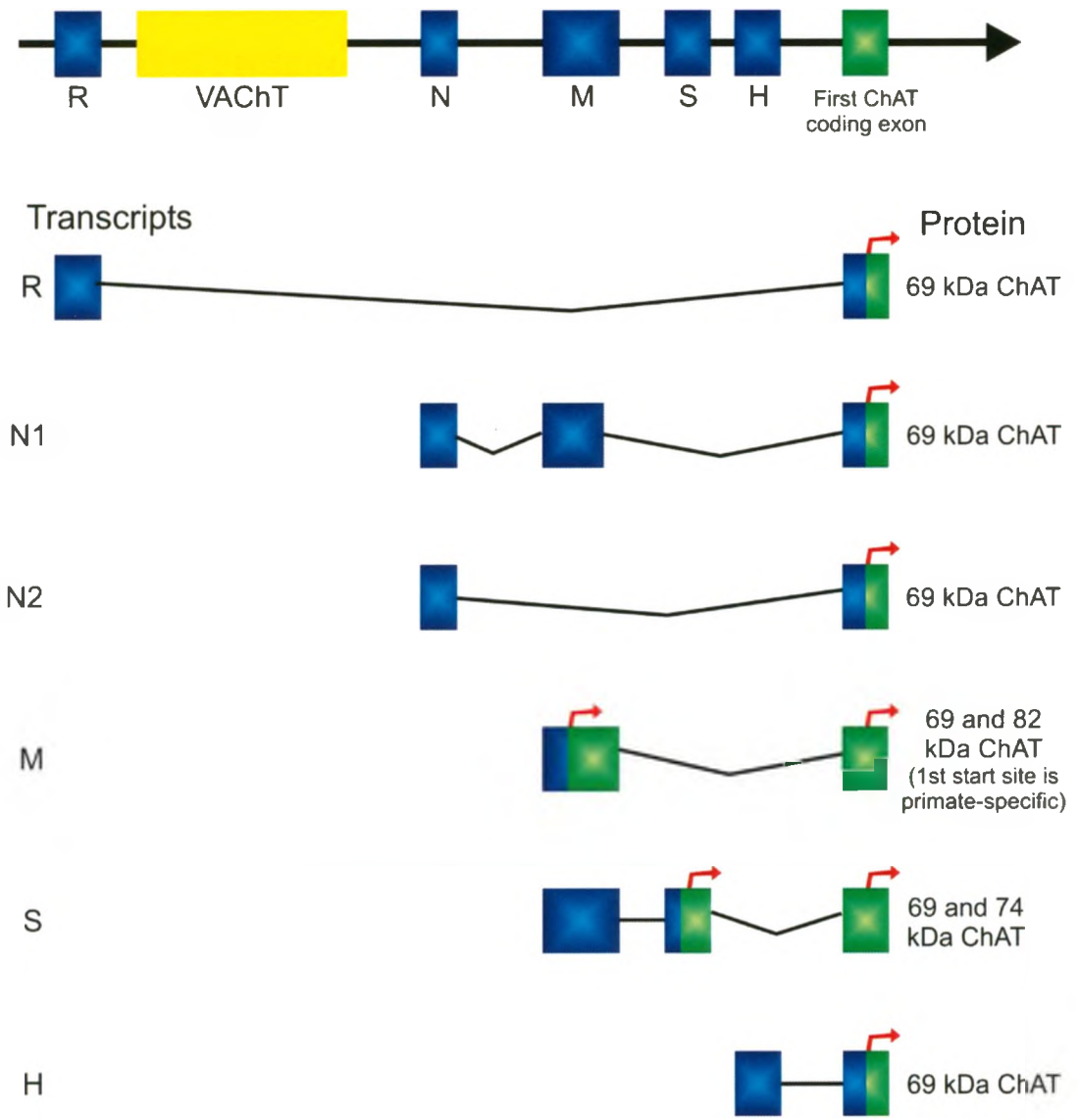

Figure 1.4: The cholinergic gene locus. The human ChAT gene is located on chromosome 10 and consists of multiple non-coding (blue) and coding (green) exons. Alternative splicing of five non-coding exons produces seven known mRNA species. The entire coding sequence for VAChT is located between the R- and N-exon, as highlighted in yellow. The various translational site starts are indicated by arrows (red). 82-ChAT is unique to primates and produced from alternative splicing of the M-transcript.

produce a 69-kDa enzyme, with the M- and S-transcripts also encoding 82- and 74-kDa proteins, respectively, due to the presence of two putative translation initiation sites (Misawa et al 1997; Oda et al 1992; Ohno et al 2001). The 82-kDa ChAT protein (82-ChAT) differs from the 69-kDa ChAT protein (69-ChAT) as it has a 118 residue amino terminal extension. Although the M-transcript is found in both primates and rodents, the rodent form lacks the first translation initiation site thus preventing production of 82-ChAT. Gill et al (2003) have shown that 69- and 82-ChAT share a nuclear localization signal (NLS) motif that allows shuttling of ChAT between the nucleus and cytoplasm. 82-ChAT has an additional NLS in the first nine residues which gives it a predominantly nuclear localization (Resendes et al 1999).

The regulatory elements important for production of different ChAT proteins have not yet been identified. However, a neuron-restrictive silencer element (NRSE) and cholinergic-specific enhancer region have been found in the rat ChAT promoter that may be important in directing the cholinergic expression of ChAT in the CNS (Lonnerberg et al 1996). Post-translational regulatory mechanisms such as phosphorylation are important in modifying ChAT catalytic activity, subcellular localization and interaction with other proteins (Schmidt and Rylett, 1993; Cooke and Rylett 1997; Dobransky et al 2001, 2003, 2004).

The 82-ChAT protein is unique to primates and its expression and distribution in human brain and spinal cord tissue has been confirmed (Gill et al 2007). Expression of both 69- and 82-ChAT is decreased with increasing age and this loss is accelerated in AD. Additionally, the nuclear localization of both

proteins is lost and 82-ChAT found largely in the cytoplasm by the 8th decade of life in neurologically-normal subjects (Gill et al 2007). The functional significance of having different subcellular distributions of ChAT proteins in primates is unknown, and it is not known if changes in the localization or expression of ChAT are a source of increased vulnerability of primate cholinergic neurons to degeneration in AD. Gene microarray studies have suggested a role for 82-ChAT in promoting the non-amyloidogenic processing of APP (Gill et al, unpublished observation). Thus, a loss of nuclear ChAT may have important implications in the pathology of AD and further investigations would allow better characterization of this role.

1.5 *Study*: Effect of 82-ChAT on Aβ pathology

Hypothesis:

1. Aβ production is elevated in E14-17 cortical cultures of the APP/PS1 transgenic mouse model of AD compared to non-transgenic littermates.
2. Human 82-ChAT promotes non-amyloidogenic processing of APP.

Specific aims of my thesis research are to:

1. Characterize Aβ production and the levels of APP processing enzymes in primary cortical neuronal cultures from embryonic day 14-17 (E14-17) APP/PS1ΔE9 (APP/PS1) double transgenic mice compared to non-transgenic littermates.

2. Determine if expression of 82-ChAT in SH-SY5Y neuroblastoma or primary neuronal cultures alters APP metabolism and Aβ production.

Rationale:

1. The APP/PS1 mouse model is a commonly used model to study pathogenesis of AD. The progression of Aβ pathology in these mice has been well characterized, with Aβ deposits seen as early as 4 months of age and Aβ load increasing up to 12 months of age. The relatively early onset of Aβ production and the extensive plaque burden seen in these mice provides a powerful model for the study of the role of Aβ in AD pathology. However, the Aβ production and pathology associated with primary embryonic cultures prepared from APP/PS1 mice has not yet been characterized. This experimental model could be a valuable tool for *in vitro* studies aimed at understanding cellular pathways involved in AD and initial testing of potential treatment strategies. The goal of this study is to determine if primary cortical cultures from APP/PS1 mice are a sufficient model to study modulation of APP processing to be used for studies of the effects of 82-ChAT on Aβ production.
2. 82-ChAT is a protein unique to primates that is found primarily in nuclei of cholinergic cells. The functional significance of this subcellular distribution is unknown. 82-ChAT protein levels decrease with increasing age and its subcellular distribution shifts with less of the protein being located in the nucleus. This effect is more pronounced in mild cognitive impairment and

AD. Following these observations, gene microarray studies were carried out to determine if expression of 82-ChAT in IMR32 cells alters mRNA levels of genes that are associated with AD. It was found that 82-ChAT altered mRNA levels of proteins associated with APP metabolism in a manner that promotes non-amyloidogenic processing of APP. The goal of the present study was to identify if expression of 82-ChAT alters Aβ production from cortical neurons cultured from E14-17 embryonic APP/PS1 mice and if this is associated with changes in expression of proteins involved in APP metabolic pathways in SH-SY5Y human neuroblastoma cells.

Outcome:

1. ELISA measurements demonstrated that significant $A\beta_{1-42}$ was released into cell culture media of E14-17 cortical cultures from TG APP/PS1 mice compared to NTG littermate controls at 8 DIV and this continued to rise at 11 DIV. At 8 DIV, human APP/Aβ was detected throughout neuronal perikarya and processes by labelling with an antibody recognizing the first 16 residues of human Aβ. Co-labelling with an $A\beta_{1-42}$ antibody detected similar areas of the cell but involved more punctuate staining. mRNA and protein levels of APP were significantly elevated in TG mice at 8 DIV compared to NTG controls. CDK5 and P35 levels were reduced but this did not reach the level of statistical significance. ADAM10 and BACE1 were largely unchanged in TG mice. Overall, the elevated levels of $A\beta_{1-42}$

in E14-17 cortical cultures of TG mice indicate that this is an adequate model for studying Aβ pathology. The elevation in $A\beta_{1-42}$ found is not associated with changes in APP processing, but rather an increase in total APP levels.

2. In SH-SY5Y cells and 8 DIV cortical cultures of APP/PS1 mice, 82-ChAT was successfully expressed in nuclei and displayed significant ChAT enzymatic activity. An approximate transduction efficiency of 50% was obtained in primary cortical cultures. Overall, 82-ChAT expression resulted in a 20% reduction in total soluble $A\beta_{1-42}$ released into media of TG mice cells compared to GFP control. This may have been due to direct effects on enzymes involved in APP processing, as a trend towards elevated ADAM10 mRNA levels were found. However, changes in BACE1 protein but not mRNA levels were significantly different with 82-ChAT expression, indicating that 82-ChAT may modulate mRNA of other regulatory proteins which are involved in post-translational modification or trafficking of BACE1. This was consistent with results in SH-SY5Y cells where a significant reduction in BACE1 mRNA was found in one 82-ChAT clone, while both clones had increased levels of ADAM10. CDK5 and P35 levels were mostly reduced with 82-ChAT expression. In contrast, a significant increase in CDK5 and P35 protein levels was found in TG mice. This was unexpected, but indicates that the reduction in $A\beta_{1-42}$ with 82-ChAT expression was not associated with changes in CDK5 and P35 levels.

CHAPTER TWO: MATERIALS AND METHODS

2.1 Materials

Most chemicals were purchased from Sigma-Aldrich (St. Louis, MO, USA) at the highest purity available. SH-SY5Y and HEK 293 cells were obtained from American Type Culture Collection (Manassus, VA, USA). Invitrogen (Burlington, ON, Canada) supplied fetal bovine serum (FBS), and culture media and reagents. The chicken egg white trypsin inhibitor was purchased from Roche (Mississauga, ON, Canada). Enhanced ChemiLuminescence (ECL) immunoblot reagents were obtained from GE Healthcare Life Sciences (Baie d'Urfé, QC, Canada). The REDExtract-N-Amp Tissue PCR Kit for genotyping from mouse tail snips and GeneElute Kit for isolation of RNA were purchased from Sigma-Aldrich. The iScript cDNA Synthesis Kit and iQ SYBR Green Kit for real-time quantitative PCR were supplied by Bio-Rad (Mississauga, ON, Canada). Primary antibodies for immunoblots include anti-CDK5 (C-8), anti-P35 (C-19), and anti-ADAM10 (A-3) antibodies purchased from SantaCruz Biotechnology Inc. (Santa Cruz, CA, USA), anti-BACE1 (C-term) from Abcam (Cambridge, MA, USA), anti-APP (22C11) from Millipore (Billerica, MA, USA) and anti-human Aβ/APP (6E10) from Covance (Princeton, NJ, USA). For immunocytochemistry, anti-NeuN (A60) antibody was purchased from Millipore and secondary AlexaFluor conjugated antibodies were purchased from Invitrogen. Polyclonal antibodies to ChAT were raised in rabbits against a peptides specific for human ChAT (Genemed Synthesis, San Antonio, Texas, USA). The CTab antibody was generated against

a peptide (CEKATRPSQGHQP) at the C-terminus of human ChAT and recognizes both 69- and 82-kDa forms of the human enzyme. The peptide was conjugated to maleimide-activated keyhole limpet haemocyanin at the N-terminal cysteine residue to enhance immunogenicity. ChAT-specific immunoglobulins were affinity-purified from crude antibody containing serum on NHS-Sepharose affinity chromatography columns (GE Healthcare Life Sciences) to which the peptides had been coupled. Specificity for these antibodies to ChAT has been described previously (Dobransky et al 2000). Polyclonal rabbit anti-$A\beta_{1-42}$ antibody was generated against a peptide at the C-terminus of $A\beta_{1-42}$ (GGVVIA) which is also available commercially from Millipore.

2.2 Plasmid transfection and generation of 82-kDa ChAT stable cell lines

The full-length cDNA for the M transcript of ChAT ligated to pSport was obtained as a gift from Dr. H. Misawa (University College London, London, UK). The M-ChAT mRNA contains two translation initiation sites that can lead to the production of both 69- and 82-ChAT proteins. To prepare a cDNA that encodes only the 82-ChAT protein, the second translation initiation methionine [Met-119] was mutated to an alanine residue. This cDNA was ligated to the mammalian expression vector pcDNA3.1(+) to yield the 82-ChAT plasmid.

SH-SY5Y neuroblastoma cells were transfected with the 82-ChAT construct using Lipofectamine 2000. Stable transformants (referred to as 82-ChAT cells) were selected with 500 µg/ml G-418 (Geneticin) for 4 weeks, and subsequently maintained in Dulbecco's modified Eagle medium (DMEM), 10%

FBS, 0.1% gentamycin, and 100 µg/ml G-418. Cells were treated with retinoic acid for 48 h to enhance the neuronal phenotype and induce differentiation towards cholinergic properties. All studies in SH-SY5Y cells were performed using two clones that stably express 82-ChAT as demonstrated in the *Results* section.

2.3 Animals and genotyping

The APP/PS1 double transgenic mouse model used in these studies was available commercially at Jackson Laboratories (Bar Harbor, ME, USA). This model was generated by co-injection of two expression plasmids (chimeric mouse/human APP_{695} with the Swedish mutation and human PS1 carrying a deletion in exon 9) into B6C3HF2 pronuclei, allowing insertion of both transgenes at a single locus. The founder line was maintained as a hemizygote by crossing to B6C3F1/J mice and transgenic mice were backcrossed to C57BL/6J mice for at least 8 generations. For these studies, male hemizygous and female wild-type (C57BL/6J) mice were maintained under standard housing conditions at the University of Western Ontario animal vivarium according to the Canadian Council on Animal Care guidelines (Appendix A). Breeding involved mating hemizygous male mice with wildtype females to produce transgenic (TG) and non-transgenic (NTG) littermates. Pregnancy was estimated by weight and females were sacrificed at embryonic day 14-17 (E14-17).

Genotyping of individual mouse embryos for the presence of the transgenes was performed on genomic DNA from tail clippings by PCR

amplification. Reactions contained primers (Table 2.1) specific for each of the two transgenes. Amplification of endogenous mouse FLOXG was used as an internal control for the success of the PCR reaction. The amplified DNA was then loaded directly onto a 1% agarose gel and visualized using ethidium bromide. Embryos were considered to be NTG if only the internal control was detected and to be TG when there was also amplification of both transgenes.

Table 2.1: Primers used for genotyping of APP/PS1 embryos

Target	Primers	Product Size
APP	For: GAC TGAC CAC TCG ACC AGG TTC TG Rev: CTT GTA AGT TGG ATT CTC ATA TCC G	350 bp
PS1	For: AAT AGA GAA CGG CAG GAG CA Rev: GCC ATG AGG GCA CTA ATC AT	608 bp
FLOXG	For: GAG AGT ACT TTG CCT GGG AGG A Rev: GGC CAC AGT AAG ACC TCC CTT G	171 bp

2.4 Cortical neuron cultures

Primary cortical neurons were prepared from mice at E14-17. Cerebral cortices from brains of individual embryos were dissected, then processed and plated separately. Tissues were dissociated by trypsinization at 37°C, and then triturated in a DNAse solution containing chicken egg white trypsin inhibitor. Cells were suspended in Neurobasal Medium containing B_{27} supplement, N_2 supplement, penicillin/streptomycin, and L-glutamine, then cells were seeded onto poly-L-ornithine coated cell culture dishes and incubated in a humidified 5% CO_2/95% air atmosphere at 37°C for 8 days *in vitro* (DIV). The results of the

genotyping performed on tail clippings from each embryo were used to assign cultures to TG and NTG groups post-hoc.

2.5 Adenoviral gene delivery system

Full-length human 82-ChAT cDNA in the pcDNA3.1 vector was used as a template for creation of the plasmid required for preparation of an adenovirus to be used to transduce neurons for expression of 82-ChAT. To accomplish plasmid preparation, an EcoRI (GAATTC) site was added to the amino-terminus and BglII (GATCT) site to the carboxyl-terminus by PCR. Following digestion of the altered plasmid with these enzymes, the resulting DNA fragment encoding 82-ChAT was ligated into the pDC316 shuttle vector which contained the loxP site necessary for recombination into the adenoviral genome.

HEK 293 wt cells maintained in Minimum Essential Medium (MEM) containing 10% FBS and 0.1% gentamycin were used for the generation and amplification of the adenoviruses. These cells provide the E1 gene that is necessary for viral replication and which was deleted from the Ad5 genomic sequence. This gene is not provided in primary neuronal cultures which therefore allows for transient expression of heterologous proteins without viral replication.

The recombinant adenoviral vector containing the human 82-ChAT sequence was obtained using the Cre/loxP system as described previously (Ng et al 1999; Figure 2.1). The shuttle vector and the adenoviral genomic plasmid (Ad5 E1-deleted adenovirus) were co-transfected into HEK 293 cells using the calcium phosphate method. Cre recombinase catalyzed the site-specific

recombination by recognition of the loxP sites. After 10 DIV, cells and media were harvested and all adenovirus was collected from cells by performing three freeze-thaw cycles and pelleting the debris. The adenovirus was aliquoted and stored at -80°C. An adenovirus was also generated that expresses GFP to be used in experiments as a negative control.

All adenovirus stocks were quantified by infecting HEK 293 cells and staining for the adenoviral hexon protein using the Adeno-X Rapid Titer Kit by Clontech (Mountain View, CA, USA), according to the manufacturer's instructions. Each stained cell corresponded to an infectious unit. The number of infected cells in a given area were counted and used to determine the total number of infectious units (ifu) in the adenoviral stocks. The multiplicity of infection (MOI), the number of ifu per cell plated, needed to obtain over-expression of human 82-ChAT in 50% of neurons was determined to be 50. Based on the results from the titration, an MOI of 50 was used for GFP adenovirus as a negative control. All neuronal cultures were exposed to the adenoviruses for 48 h.

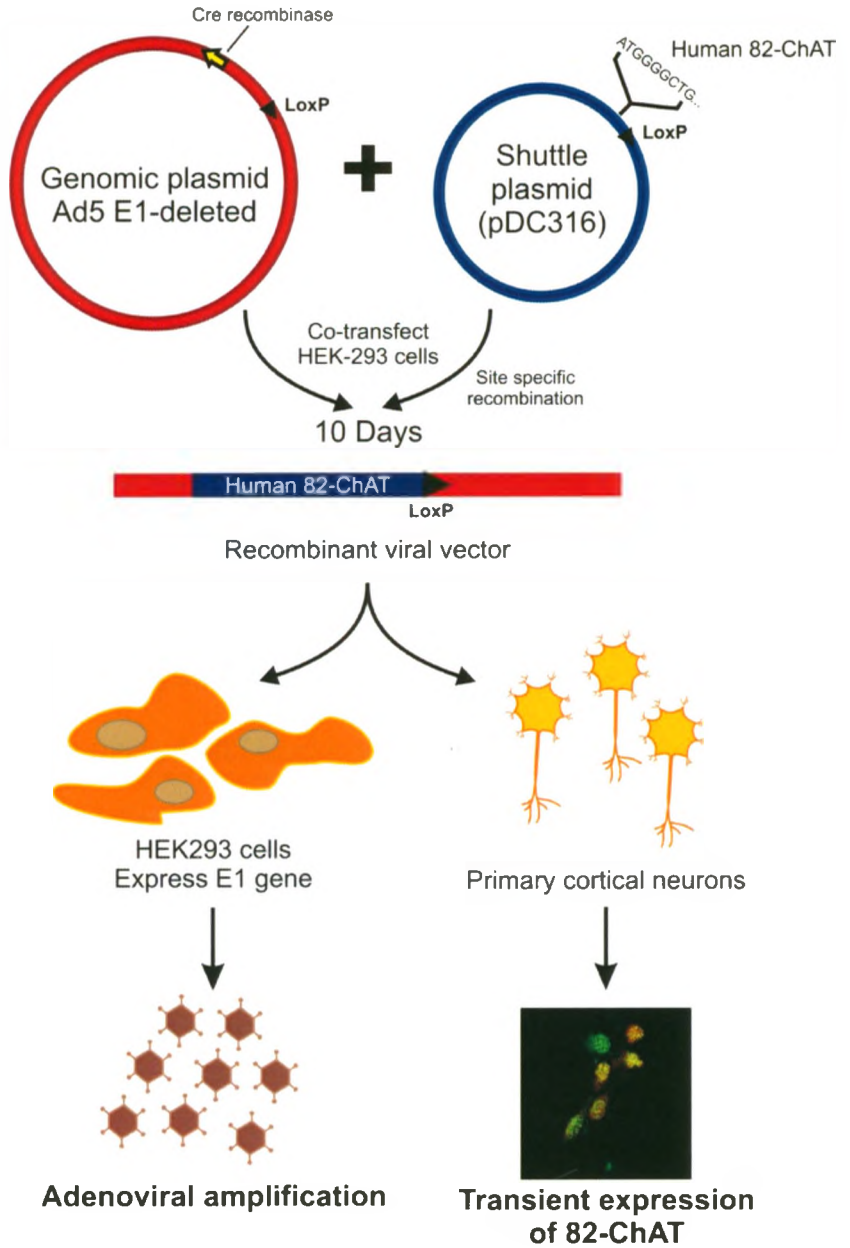

Figure 2.1: Adenoviral gene delivery system for expression of 82-ChAT in primary cortical neurons. Full-length human 82-ChAT was ligated into the pDC316 shuttle vector. Co-transfection with the Ad5 adenoviral plasmid (E1 deleted) into HEK293 cells allowed insertion of 82-ChAT into the adenoviral genome by site-specific recombination. The recombinant viral vector was further amplified in HEK293 cells that provide the E1 enzyme necessary for replication. In contrast, this enzyme was not provided in primary cortical neurons and the adenovirus could be used for transient expression of 82-ChAT proteins.

2.6 Localization of 82-ChAT in by immunocytochemistry

Cortical neurons were seeded on poly-l-ornithine-coated MatTek confocal dishes (0.2 x 10^6 cells/dish). Adenoviruses were added directly to culture media on the cells 48 h prior to processing for antibody-labeling. For SH-SY5Y clones, cells were seeded on collagen-coated MatTek confocal dishes (0.3 x 10^6 cells/dish) at 48 h prior to processing for antibody-labeling. Images of fixed cells were obtained using a Zeiss LSM510-Meta laser scanning confocal microscope with a Zeiss 63 X 1.4 NA oil-immersion lens. All antibody-labeling of cells was performed at room temperature. Cells were washed twice with 1 x phosphate buffer saline (PBS, pH = 7.4) and then fixed for 30 min in 4% formaldehyde-PBS. Fixed cells were treated with blocking solution (PBS containing 0.05% Triton X-100 and 3% normal goat serum) for 1 h to block non-specific binding sites and permeabilize the cells. Primary neurons were co-labeled for human ChAT (CTab, 1:2000) and neuronal nuclear protein (NeuN, 1:100) by incubating fixed cells in blocking buffer containing both primary antibodies for 1 h. GFP-virus transduced cells were only labeled with the NeuN antibody. SH-SY5Y clones were only labeled with the CTab antibody. Following incubation with the primary antibodies, cells were washed to remove any unbound antibody and then incubated with secondary antibodies for 1 h. The AlexaFluor 488 conjugated goat anti-rabbit IgG antibody (1:500) was used to detect ChAT and AlexaFluor 633 conjugated goat anti-mouse IgG antibody (1:1000) was used to detect NeuN. Expression of 82-ChAT was determined by dual excitation (488 and 633 nm), and emission (band pass 505-530 for AlexaFluor 488 or GFP; 650 long pass for AlexaFluor 633) filter

sets. Non-specific binding from secondary AlexaFluor conjugated antibodies was determined from samples labeled in the absence of primary antibodies.

2.7 ChAT activity assay

ChAT specific activity was determined in a modified method described previously by Fonnum (1969). Cells cultured in 35 mm dishes were washed with PBS and lysed for 30 min on ice in 50 mM Tris-HCl (pH = 7.5) containing 150 mM NaCl, 0.5% Triton X-100, 100 mM AEBSF, 10 mg/ml leupeptin, 25 mg/ml aprotinin, 10 mg/ml pepstatin, and 700 units/ml DNAse I. For each sample, triplicate 10 µl aliquots of total cell lysate were incubated with 10 µl of substrate solution (0.1 M sodium phosphate buffer [pH = 7.4], 0.1% bovine serum albumin, 0.2 mM eserine hemisulphate, 300 mM NaCl, 4 mM choline iodide, and 0.2 mM [3H]acetyl-CoA tri-lithium salt (10 mCi/mmol) for 15 min on ice. Activity of ChAT was measured by isolation of [^{3}H]ACh using a liquid cation extraction method with 10 mg/ml sodium tetraphenylboron in 3-heptanone. Specific activity of ChAT was calculated by subtracting background activity in the absence of added choline and normalized to sample protein content.

2.8 SYBR green quantitative real-time PCR

SH-SY5Y cells or primary neurons cultured in 60 mm dishes were washed with PBS and total RNA was isolated. mRNA was reverse transcribed and first-strand cDNA was amplified in triplicate on the Bio-Rad CFX96 system. Forward and reverse primers for each gene are listed in Table 2.2. SYBR green was the

detection method used and all genes were normalized to GAPDH. Fold-change was calculated by the ΔΔCt method relative to the signal from either empty vector expressing SH-SY5Y cells or NTG littermates in untreated neurons. For neuronal cultures involving adenoviral treatments, fold-change was calculated relative to GFP-expressing cells. All statistical analyses were performed on normalized Ct values prior to the determination of fold-change values. Primer efficiency and amplification of single PCR products were confirmed as described in the *Results* section.

Table 2.2: List of real-time PCR primers

Gene	Species	Primers
CDK5	Human	For: ATG GTG ACC TCG ATC CTG AG Rev: GGC TTC AGG TCC CTG TGT AG
CDK5	Mouse	For: TGC TGA GGT GGT CAC GCT GT Rev: AGC CTG GCC ACT GGG GTT CA
P35	Human	For: CTT CTC CGA CCT GAA GAA CG Rev: ATG CAT TGA ATC CTT GAG CC
P35	Mouse	For: ACG TAC TCA CAG AGG TGG GG Rev: GCA GCA GGA TGT GAG GAT GG
APP	Human	For: CCG CTC TGC AGG CTG TT Rev: TTC TGT TCT GCG CGG AC
APP	Mouse	For: AAG AAC TTG CCC AAA GCT GA Rev: GTC TCT CAT TGG CTG CTT CC
BACE1	Human	For: CTT TGT GGA GAT GGT GGA CA Rev: TGC AAA GTT ACT GCT GCC TG
BACE1	Mouse	For: TGG ACT GCA AGG AGA CGG AG Rev: AAC AGT GCC CGT GGA TGA CT
ADAM10	Human	For: ATG GGA GGT CAG TAT GGG AAT C Rev: TTT GGC ACG CTG GTG TTT TTG
ADAM10	Mouse	For: GCA CCT GTG CCA GCT CTG AT Rev: GCC CAC CAG TGA GCC ACA AT
GAPDH	Human	For: TGT TGC CAT CAA TGA CCC CTT Rev: CTC CAC GAC GTA CTC AGC G
GAPDH	Mouse	For: TTG TGA TGG GTG TGA ACC ACG AGA Rev: CAT GAG CCC TTC CAC AAT GCC AAA

2.9 Human $A\beta_{1-42}$ ELISA assay

Total levels of human $A\beta_{1-42}$ produced in cell culture medium from cortical cultures of individual embryos were measured using the human $A\beta_{1-42}$ ELISA kit (Invitrogen) according to the manufacturer's protocols.

2.10 Immunoblots for Aβ

The presence of monomeric and oliogomeric aggregates of Aβ in media of neurons cultured from APP/PS1 mouse embryos was determined by immunoblotting. Media from individual embryos was collected and protein degradation was inhibited by addition of a 10x lysis buffer (500 mM Tris-HCl [pH = 7.5] 1.5 M NaCl, 5% Triton X-100) containing a 10x concentration of protease inhibitors (1 mM AEBSF, 100 µg/ml leupeptin, 250 µg/ml aprotinin, and 100 µg/ml pepstatin). Aliquots of each sample were taken for quantification using the human $A\beta_{1-42}$ ELISA assay. To concentrate samples for analysis by SDS-PAGE, media samples were transferred to Amicon Ultra-4 centrifugal filter devices (Millipore) and centrifuged at 4,000 x g for 90 min. The resulting concentrated samples (50 µl) were incubated at 55°C for 10 min in tris-tricine sample buffer (2% SDS, 40% glycerol, 200 mM Tris-HCl [pH = 6.8], 0.04% Coomassie blue G-250, and 2% β-mercaptoethanol). Samples were loaded on 10%/16.5% SDS-PAGE tris-tricine gels and transferred to pure nitrocellulose membranes. Membranes were blocked in 8% non-fat dry milk in wash buffer (PBS and 0.05% Triton X-100) for 1 h, then incubated overnight at 4°C in primary antibody (human Aβ/APP [6E10], 1:2,000) in wash buffer containing 8% milk. Membranes were

washed and incubated with horseradish peroxidise conjugated sheep anti-mouse IgG secondary antibody (1: 2,000) in wash buffer containing 8% milk for 1 h. After washing, immunoreactive bands were detected by chemiluminescence using the ECL kit.

2.11 $A\beta_{1-42}$ levels by immunocytochemistry

Digital images were obtained using the Zeiss LSM10-Meta laser scanning confocal microscope using a Zeiss 63 X 1.4 NA oil-immersion lens. All incubations were performed at room temperature. Cortical neurons plated on MatTek confocal dishes (0.2×10^6 cells/dish) were washed with PBS and fixed in 4% formaldehyde-PBS for 30 min. Cells were washed and incubated for 1 h in blocking buffer (0.05% Triton-X-100 and PBS containing 3% goat serum). Cells were then incubated with primary antibodies rabbit anti-$A\beta_{1-42}$ (1:1,000) and mouse anti-human Aβ/APP (6E10, 1:1,000) for 1 h. After washing, cells were incubated in AlexaFluor 488 conjugated goat anti-rabbit and AlexaFluor 633 conjugated goat anti-mouse secondary antibodies for 1 h. Following washing, neuronal expression of $A\beta_{1-42}$ was detected microscopically using dual excitation (488 and 633 nm) and emission (505-530 band pass for AlexaFluor 488 and 650 long pass for AlexaFluor 633) filter sets.

2.12 Immunoblots of endogenous protein levels

Cells cultured on 35 mm dishes were washed with PBS and lysed for 30 min on ice in 50 mM Tris-HCl (pH 7.5) containing 150 mM NaCl, 0.5% Triton X-

100, 0.1 mM AEBSF, 10 µg/ml leupeptin, 25 µg/ml aprotinin, 10 µg/ml pepstatin and 700 units/ml DNAse I. Protein concentration was determined using the Bradford assay (BioRad), using bovine serum albumin as a standard. Aliquots of cell lysates containing 50 µg of protein were incubated at 100°C for 5 min in SDS sample buffer (2% SDS, 10% glycerol. 0.1 M sodium phosphate buffer, pH 7.2, 0.001% bromophenol blue, and 7.5% β-mercaptoethanol). Sample proteins were separated on 10% SDS-PAGE gels and transferred to pure nitrocellulose membranes. Membranes were blocked in 8% non-fat dry milk in wash buffer (PBS and 0.05% Triton X-100) for 1 h, then incubated overnight at 4°C in primary antibody in wash buffer containing 8% milk. Membranes were washed and incubated with horseradish peroxidise conjugated secondary antibody in wash buffer containing 8% milk for 1 h. After washing, immunoreactive bands were detected by chemiluminescence using the ECL kit. For primary cortical neurons, immunoreactive bands were quantified by measuring pixel intensity using the Scion Image software made available by the US National Institutes of Health. Bands were normalized to actin levels to control for loading efficiency.

2.13 Data analysis

Data are presented as the mean ± SEM with *n* values representing the number of independent experiments performed on separate populations of cells. Each *n* value was obtained from multiple sample replicates in each experiment. GraphPad Prisim 5 was used to analyze the data. Statistical significance was determined by Student's *t*-tests, one-way ANOVA followed by Tukey's posthoc

multiple comparisons test or two-way ANOVA followed by Bonferroni posthoc test where appropriate (* = $p \leq 0.05$, ** = $p \leq 0.01$, *** = $p \leq 0.001$).

CHAPTER THREE: RESULTS

3.1 Confirmation of stable expression of 82-ChAT in SH-SY5Y cells

The M-transcript of human ChAT contains two translation initiation sites that can result in the production of both 69- and 82-ChAT proteins as shown by *in vitro* translation (Misawa et al 1997) and by heterologous expression in cultured cells (Resendes et al 1999). In this study, the second translation initiation methionine in cDNA encoding the human ChAT M-transcript was mutated to an alanine residue (M119→A) to preclude production of 69-ChAT. Previous studies have shown that 82-ChAT is functional when expressed in HEK293 cells and has a predominantly nuclear localization (Resendes et al 1999; Gill et al 2003). These studies were confirmed in two clones of SH-SY5Y cells that were engineered for stable expression of 82-ChAT. Figure 3.1 demonstrates that both clones express 82-ChAT (Panel B; CTab antibody) and that this enzyme is catalytically active (Panel C) with a specific ChAT activity of 24.13 ± 1.796 nmol/mg/h and 29.45 ± 9.573 nmol/mg/h for clone 1 and 2, respectively. Additionally, 82-ChAT is found predominantly in the nucleus of these neural cells with faint staining in the cytoplasm (Panel A), which is consistent with the results of previous studies. No ChAT immunoreactivity or ChAT enzymatic activity (0.7161 ± 0.5369 nmol/mg/h) is observed in cells over-expressing the empty vector alone.

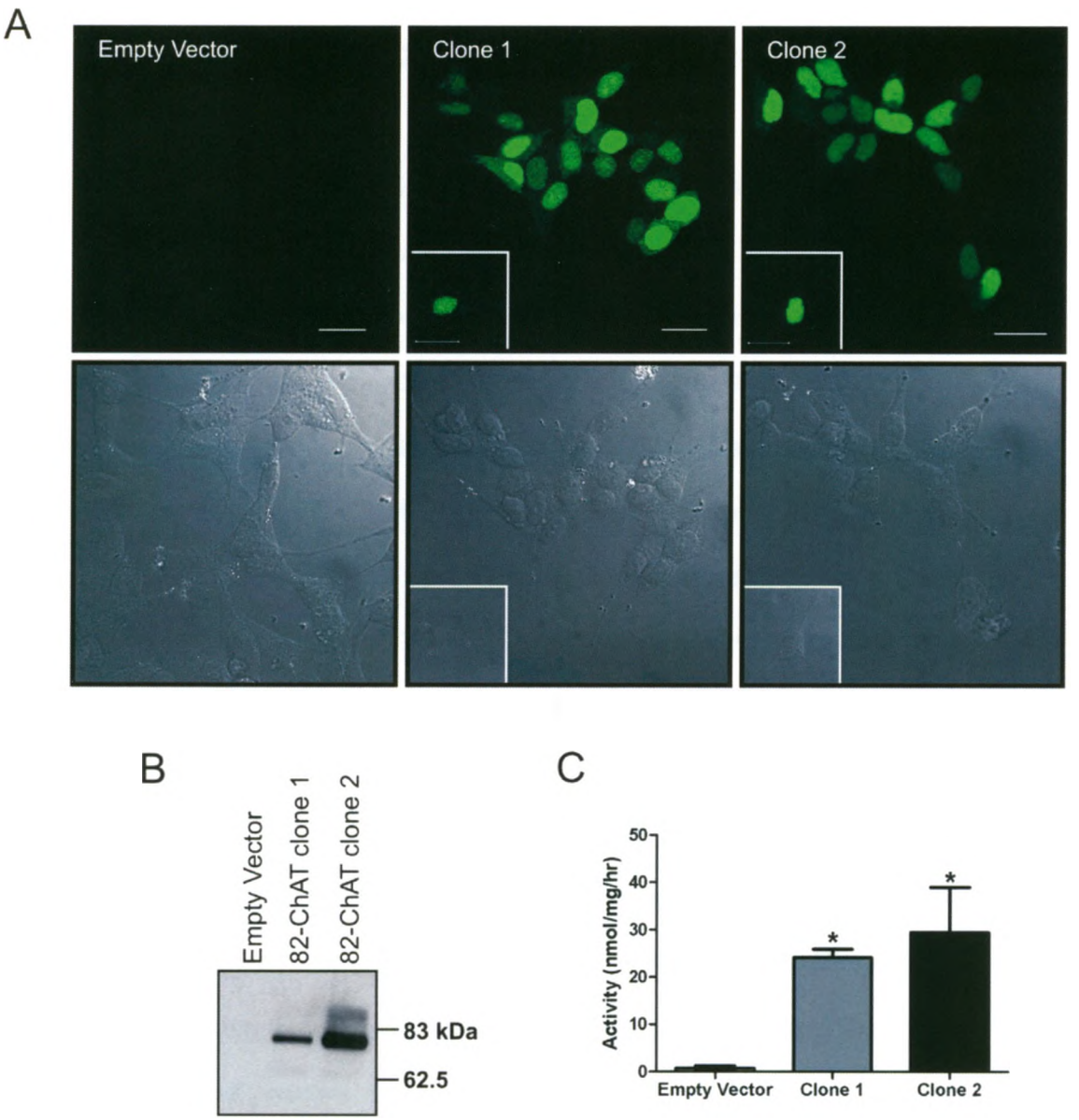

Figure 3.1: Stable expression of 82-ChAT in SH-SY5Y cells. Confocal images (Panel A) and immunoblots (Panel B) confirm high levels of expression of 82-ChAT in two different SH-SY5Y clones with a predominantly nuclear localization. Cells expressing the empty vector pcDNA3.1 are not immunoreactive with the CTab anti-ChAT antibody. 82-ChAT is functional as confirmed by the enzyme activity assay (Panel C). Scale bars represent 20 μm. For ChAT activity assay, data are expressed as mean ± SEM of 4 independent experiments, * = $p < 0.05$ compared to empty vector expressing cells.

3.2 Transient expression of 82-ChAT in primary neuron cultures from APP/PS1 mice

82-ChAT was expressed in primary cortical neurons using the adenoviral gene delivery system to transduce cells with ChAT cDNA. Images were taken of cells prior to adenoviral treatment (at 6 DIV) and after 48 h of adenovirus exposure (at 8 DIV) and are shown Figure 3.2. Cells appeared healthy in culture in the absence (Panels A and B) and presence of GFP (Panel C) or 82-ChAT (Panel D) adenoviruses (MOI of 50). Figure 3.3 demonstrates that 82-ChAT is expressed in cells (Panel D; CTab antibody) and is catalytically active (Panel E) with a specific ChAT activity of 34.64 ± 7.9 nmol/mg/hr. Immunocytochemistry was used to determine if the localization of 82-ChAT in cortical neurons is consistent with that observed in the SH-SY5Y stable clones. 82-ChAT was stained using the CTab anti-ChAT antibody and cultures were counterstained for the neuronal nuclear protein (NeuN) to distinguish neurons from non-neuronal cell types, as a small percentage of cells in culture (<10%) were non-neuronal. 82-ChAT was found to co-localize with NeuN (Panel B), indicating that it was located in nuclei of neurons. Examination of a random field of cells (Panel C) illustrated that approximately 50% of neurons in culture expressed 82-ChAT at varying levels. No immunoreactivity or ChAT enzymatic activity (1.501 ± 0.66 nmol/mg/hr) was observed in cells transduced with the GFP adenovirus as a negative control (Panels A, D and E).

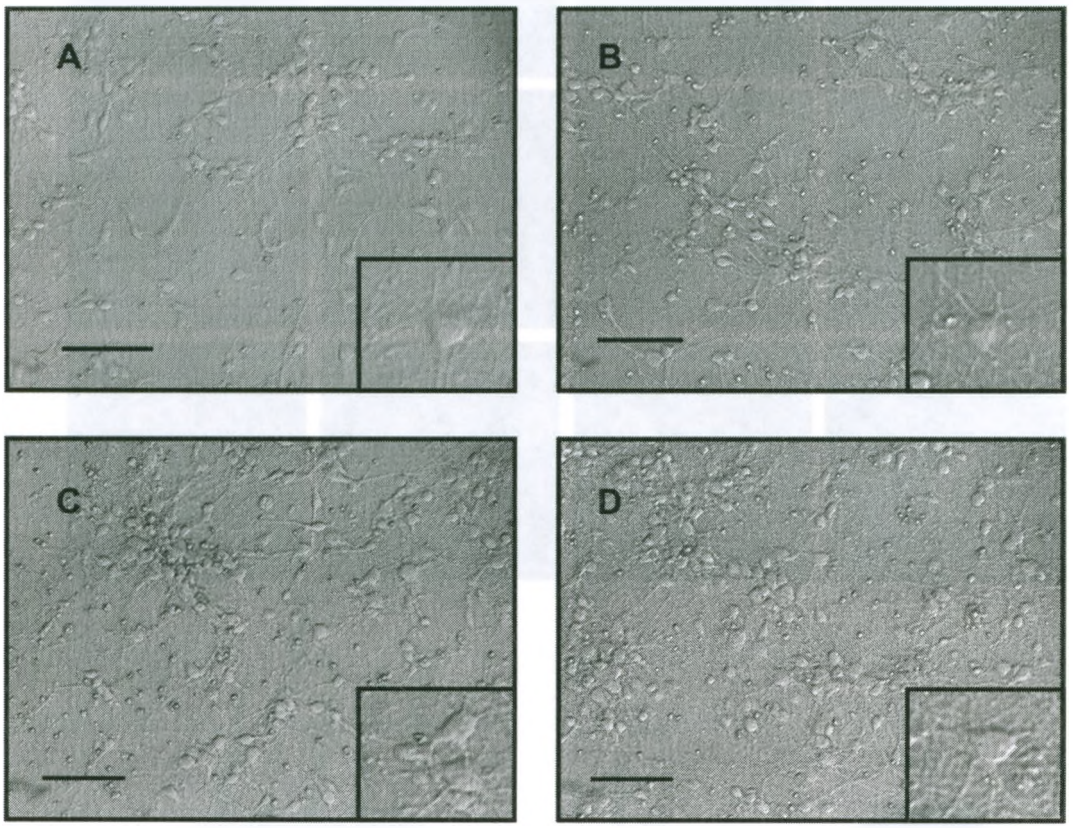

Figure 3.2: Primary cortical cultures of APP/PS1 mice. Images of cells in culture were taken prior to adenoviral treatment at 6 DIV (Panel A). At 8 DIV, cells appear healthy without treatment (Panel B) and after 48 h of transduction with GFP (Panel C) or 82-ChAT (Panel D) adenoviruses. Images were taken at 20X magnification and scale bars represent 50 μm.

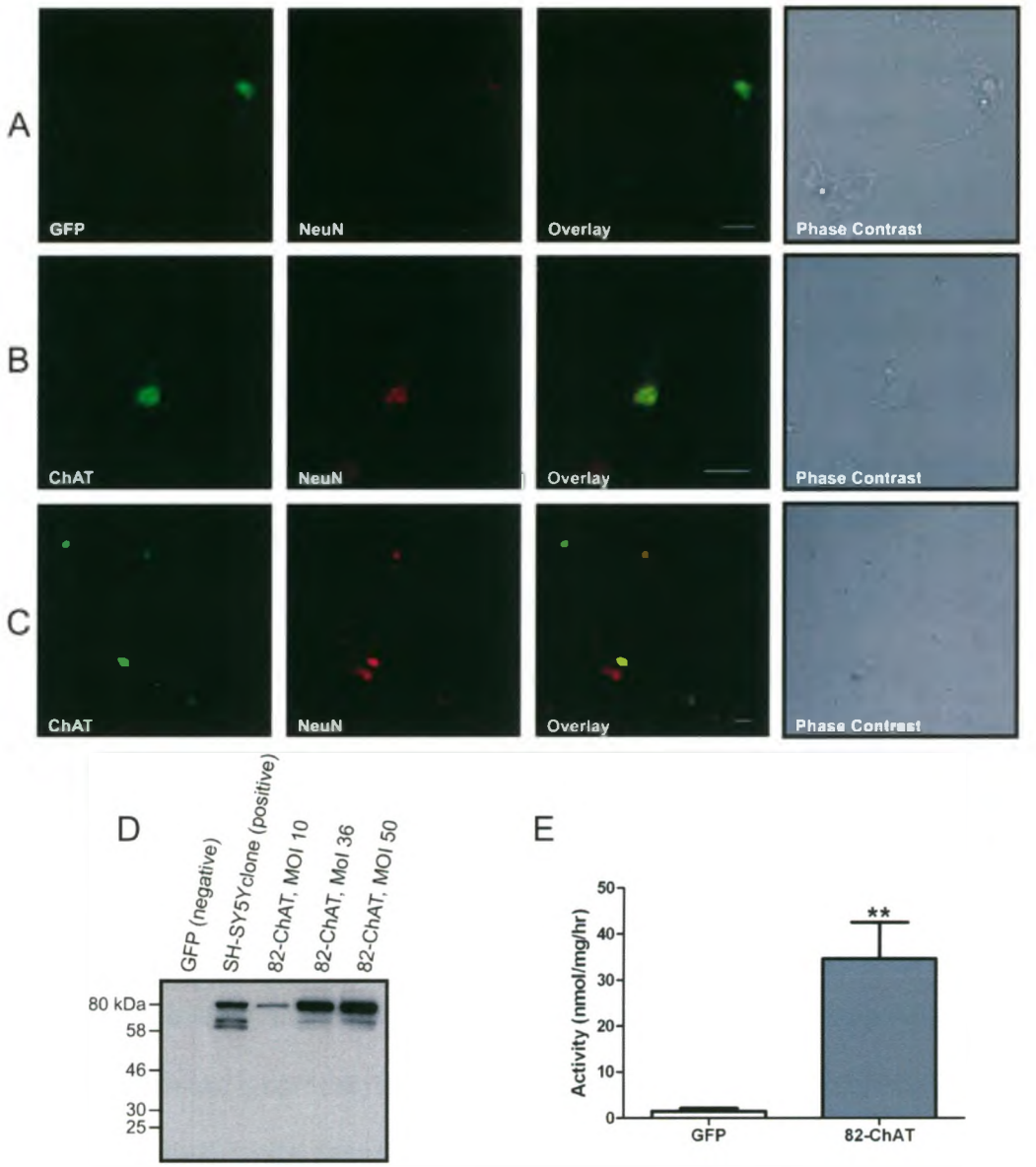

Figure 3.3: Expression of functional 82-ChAT in primary cortical neurons. 82-ChAT was expressed in primary cortical neuron cultures using an adenoviral gene delivery system. Levels of 82-ChAT with 48 h of exposure to increasing amounts of adenovirus are shown (Panel D). Neurons transduced with MOI = 50 have significant enzyme activity (Panel E) with predominantly nuclear localization (Panel B, green) and about 50% of neurons (NeuN positive, red) expressing the protein (Panel C). Cells were also transduced with GFP adenovirus as a negative control (Panels A, D and E). Scale bars represent 20 μm. For ChAT activity, data are expressed as mean ± SEM of 5 independent experiments, ** = $p < 0.01$.

3.3 Genotyping from individual embryos of APP/PS1 mice

Breeding involved mating hemizygous male mice with wild-type females and produced hemizygous TG or NTG littermates. At approximately E14-17, pregnant females were sacrificed and neuronal cultures were prepared from cerebral cortex of embryonic mouse brains. At the same time, genomic DNA was isolated from tail clippings of each embryo and genotyping was performed as described in the *Methods* section. An example of the genotyping results from one litter of mice is shown in Figure 3.4. Embryos were identified to be NTG when a single band for FLOXG at 171 bp was observed (embryos 1, 2, 3, 5, 9). Embryos were TG when bands for each of the two transgenes were also observed; the APP PCR amplicon was at 350 bp and the PS1 PCR amplicon was at 608 bp (embryos 4, 7, 8, 10). The absence of any gene product (embryo 6) indicated that the PCR reaction was unsuccessful and was repeated.

3.4 APP/PS1 cortical cultures release significant levels of human $A\beta_{1-42}$

To determine if cortical neuron cultures prepared from brain of embryonic APP/PS1 transgenic mice are an adequate model to study cellular mechanisms involved in AD, we first characterized the levels and time course for Aβ production. To accomplish this, we used a sensitive ELISA to measure release of endogenous human $A\beta_{1-42}$ into media bathing the cortical neurons after various times in culture. In Figure 3.5, Panel A demonstrates that at 4 DIV, a small amount of Aβ was produced in cultures from TG mice compared to NTG mice (16.7 ± 7.8 versus 7.4 ± 3.2 pg/ml), but this did not reach the level of statistical

significance when analyzed by two-way ANOVA with Bonferroni post-hoc tests. At 8 DIV, the level of Aβ produced in cultures from TG mice was significantly elevated (284.8 ± 41.3 versus 5.2 ± 0.7 pg/ml) and this level continued to rise at 11 DIV (909 ± 28.2 versus 6.5 ± 0.3 pg/ml). To characterize the composition of Aβ species found in these samples of culture medium, aliquots were concentrated and immunoblots for total human Aβ were performed as described in the *Methods* section. A representative immunoblot is shown in Figure 3.5 Panel B. We were unable to detect immunoreactive bands for Aβ in lanes with either NTG or TG media samples when compared to the synthetic Aβ peptide (positive control). A single band was observed in media samples from cultures prepared from TG mice with an apparent molecular mass of approximately 100 kDa, which coincides with the sAPPα fragment released by α-secretase cleavage of APP that has been detected previously in neuron-conditioned media by immunoblotting (Zhang et al 2010). This was not observed in media from neuron cultures from NTG mice. To confirm the identity of the immunoreactive band appearing in the samples from TG mouse cultures, the immunoblot was stripped and re-probed for APP as shown in Figure 3.5 Panel C. Under these conditions, Aβ proteins could not be detected by immunoblots possibly because Aβ they are prone to aggregation and difficult to separate by SDS-PAGE.

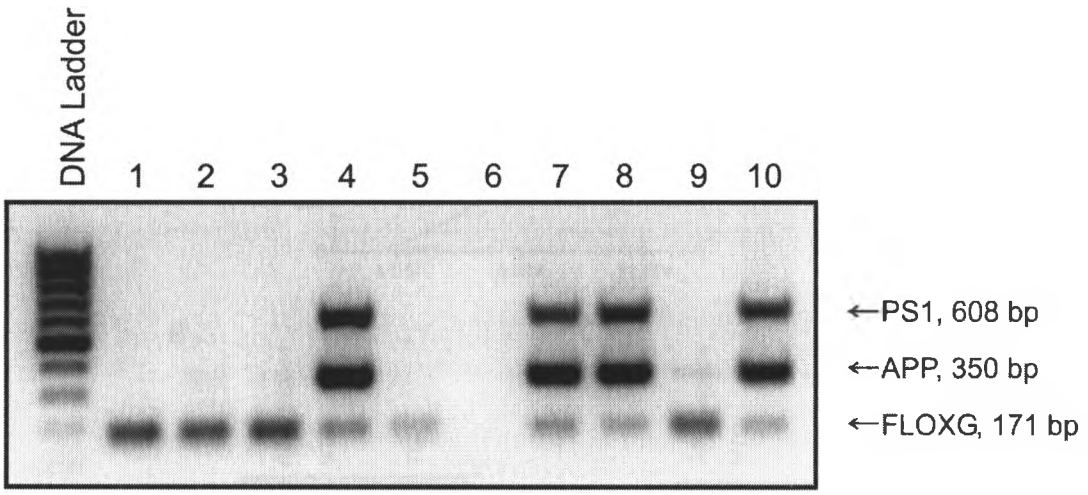

Figure 3.4: Genotyping from APP/PS1 embryonic mouse tail snips. A representative set of genotyping results from one litter that had 10 embryos is shown. Genomic DNA was amplified by PCR with primers specific for the transgenes and endogenous FLOXG. All samples with successful PCR amplification gave a 171 bp product from the endogenous FLOXG gene and transgenic embryos gave additional bands at 350 and 608 bp for APP and PS1 transgenes, respectively.

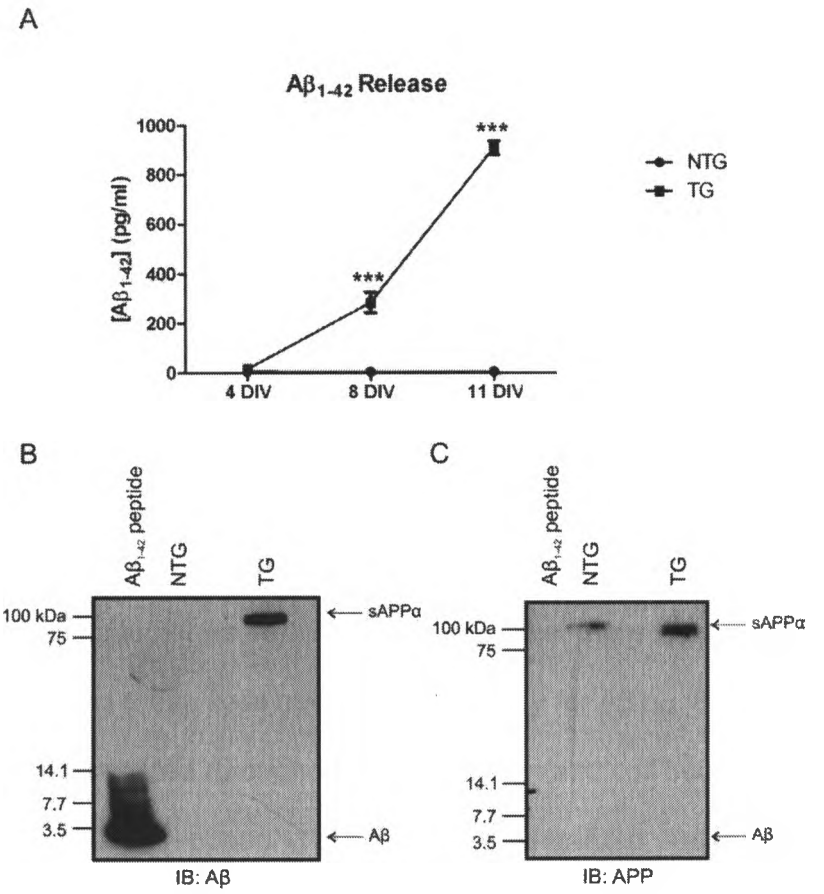

Figure 3.5: Human $A\beta_{1-42}$ is released from primary cortical cultures of APP/PS1 mice. Levels of human $A\beta_{1-42}$ produced into the media from primary cortical neurons of APP/PS1 mice were measured by ELISA. A time-dependent increase in $A\beta_{1-42}$ was observed in cultures of TG mice as compared to NTG littermate controls (Panel A). At 8 DIV, concentrated media samples were run on 10%/16.5% tris tricine gels and immunoblots for total human Aβ were performed; a representative immunoblot is shown (Panel B). Immunoreactivity was observed only in lanes containing synthetic Aβ peptide (positive control) and TG mice media where only the sAPPα fragment was detected. Reprobing for APP (Panel C), only detected immunoreactive bands for the sAPPα fragment, confirming that the band observed (Panel B) was not aggregated Aβ proteins. For ELISA, data are expressed as +/- SEM of 3-5 independent experiments, *** = $p < 0.001$.

3.5 $A\beta_{1-42}$ is found in the cell bodies and processes of APP/PS1 cortical cultures

To detect intracellular $A\beta_{1-42}$ peptides that were not released into the cell culture media we used immunocytochemistry to label human $A\beta_{1-42}$ proteins in cells at 8 DIV. Cells were double-labeled using an antibody specific to $A\beta_{1-42}$ and for human Aβ/APP. In Figure 3.6, cells from NTG mice are not immunoreactive for human Aβ/APP (red) and have some reactivity using the $A\beta_{1-42}$ antibody (green). Endogenous mouse APP levels may be detected in these cells as cross-reactivity with endogenous mouse APP has not been reported. As a result, non-specific staining could not be determined. In TG mice, there is clear staining for human Aβ/APP and these cells have more reactivity for $A\beta_{1-42}$. Both antibodies detect proteins distributed throughout the cytoplasm and cell bodies, with the $A\beta_{1-42}$ antibody staining appearing to be compartmentalized. Areas of co-localization, seen as yellow, could represent human $A\beta_{1-42}$ proteins.

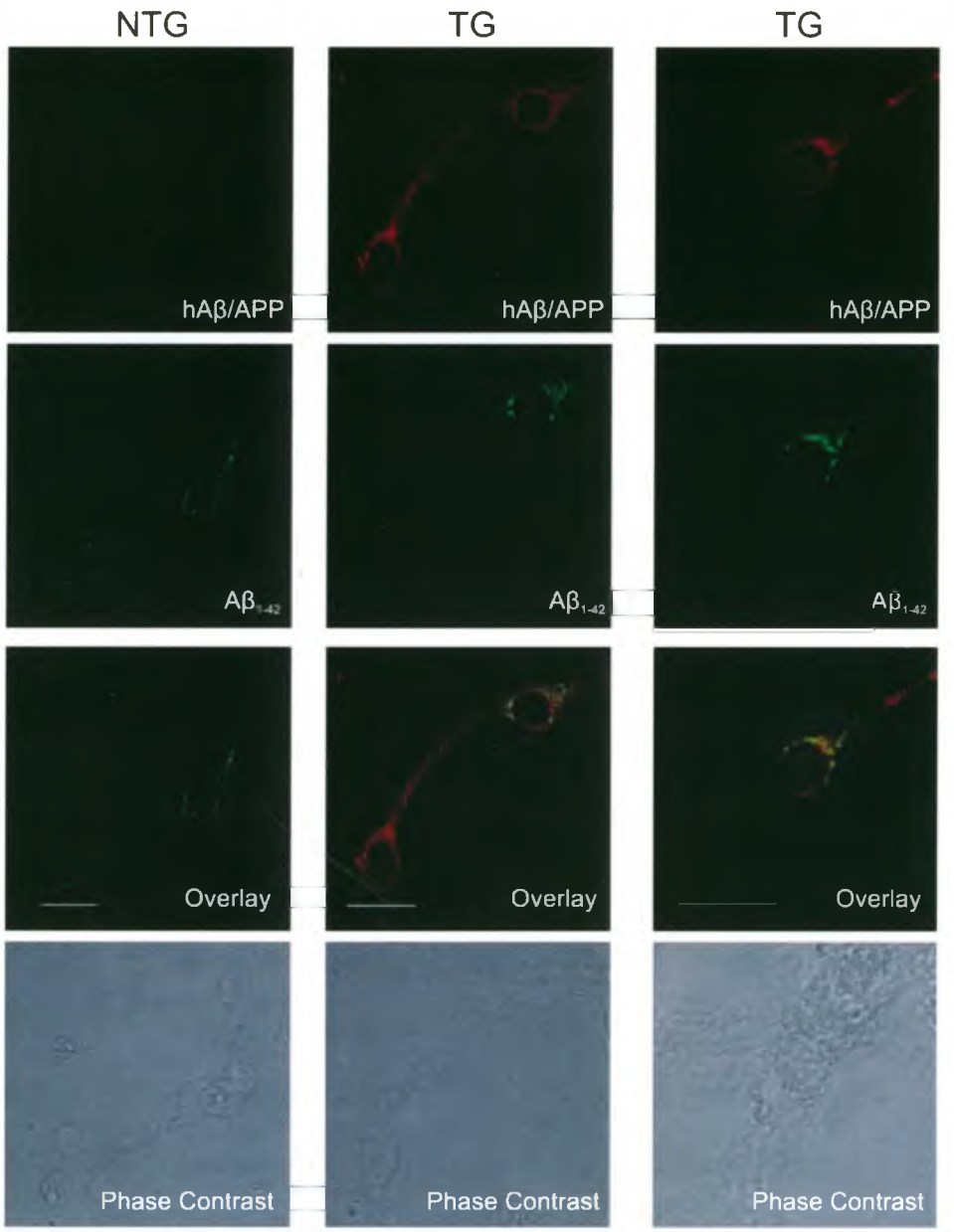

Figure 3.6: hAPP/Aβ$_{1-42}$ is found in the cytoplasm and processes of APP/PS1 mice. Primary cultures at 8 DIV were labeled using antibodies specific for Aβ$_{1-42}$ (green) and human Aβ/APP (red). NTG mice have low staining with Aβ$_{1-42}$ antibody which may represent total APP levels or background staining. No immunoreactivity from human Aβ/APP antibody is observed in NTG mice. TG mice are immunoreactive for human Aβ/APP throughout the cell bodies and processes with more intense staining for Aβ$_{1-42}$ antibody. Areas of colocalization (yellow) may represent areas where intracellular Aβ$_{1-42}$ proteins are found. Scale bar represents 20 μm.

3.6 APP processing in APP/PS1 cortical cultures

The baseline expression of genes related to APP processing was examined by assessing the mRNA and protein levels in cultured neurons at 8 DIV. The mRNA levels of APP, ADAM10, BACE1, CDK5 and P35 were evaluated by real-time PCR using primers specific to the murine genome. CDK5 has been studied extensively for its role in AD, as a possible link between Aβ pathology and NFT formation. To be activated, CDK5 must interact with its regulatory subunit, P35. Under some forms of cellular stress, calpain activation results in cleavage of P35 to P25, which is not readily degraded and constitutively activates CDK5 (Lee et al 2000). Under these conditions, CDK5 increases Aβ production by affecting APP phosphorylation and BACE1 activity (Alvarez et al 2001; Liu et al 2003; Cruz et al 2006; Wen et al 2008). CDK5 phosphorylates tau, preventing its ability to stabilize microtubules and leading to NFT formation (Patrick et al 1999; Hamdane et al 2003). This can be triggered by treatment with Aβ in cell culture models (Town et al 2002), thus providing a possible link between tau and Aβ pathology.

The quality of primers used for real-time PCR was confirmed by calculating primer efficiency and ensuring that only single amplicons were produced. Figure 3.7 summarizes the quality control results for all murine primers used. Primer efficiency was calculated by the slope of standard curves generated by plotting the concentration of serially diluted cDNA against the corresponding Ct value (Panels A and B). Melting curves were generated for each primer set by measuring fluorescence as samples were heated and bound SYBR green was

released. At the melting point, the fluorescence rapidly decreases and this point was visualized by plotting the second derivative curve. A single peak at the melting point as well as the lack of amplification in samples that lacked RNA template (no template control, NTC) indicated that no non-specific amplification was present. Also, the absence of any peaks at lower temperatures indicated that primer-dimers were not formed. Sample melting curves for APP, BACE1 and GAPDH from one experiment are given (Panel C). Additionally, PCR products were run on 1% agarose gels to visualize single amplicons by ethidium bromide (Panel D).

Protein levels were evaluated using antibodies that recognize both human and murine proteins described in the *Methods* section. Pixel intensity was normalized to actin levels to control for differences in sample loading. Figure 3.8 demonstrates that a significant increase in APP was found at the mRNA (1.5 ± 0.08) and protein (1.33 ± 0.14) level in TG mice when analyzed by two-way ANOVA with Bonferroni post-hoc test. A trend towards decreased fold-change mRNA of CDK5 (0.56 ± 0.06), P35 (0.68 ± 0.12) and ADAM10 (0.9 ± 0.11 mRNA) in TG mice were found. These were consistent with changes in protein levels (0.76 ± 0.11 for CDK5, 0.72 ± 0.15 for P35 and 0.83 ± 0.11 for ADAM10). BACE1 mRNA levels were elevated (1.21 ± 0.21) but BACE 1 protein levels were reduced (0.73 ± 0.21).

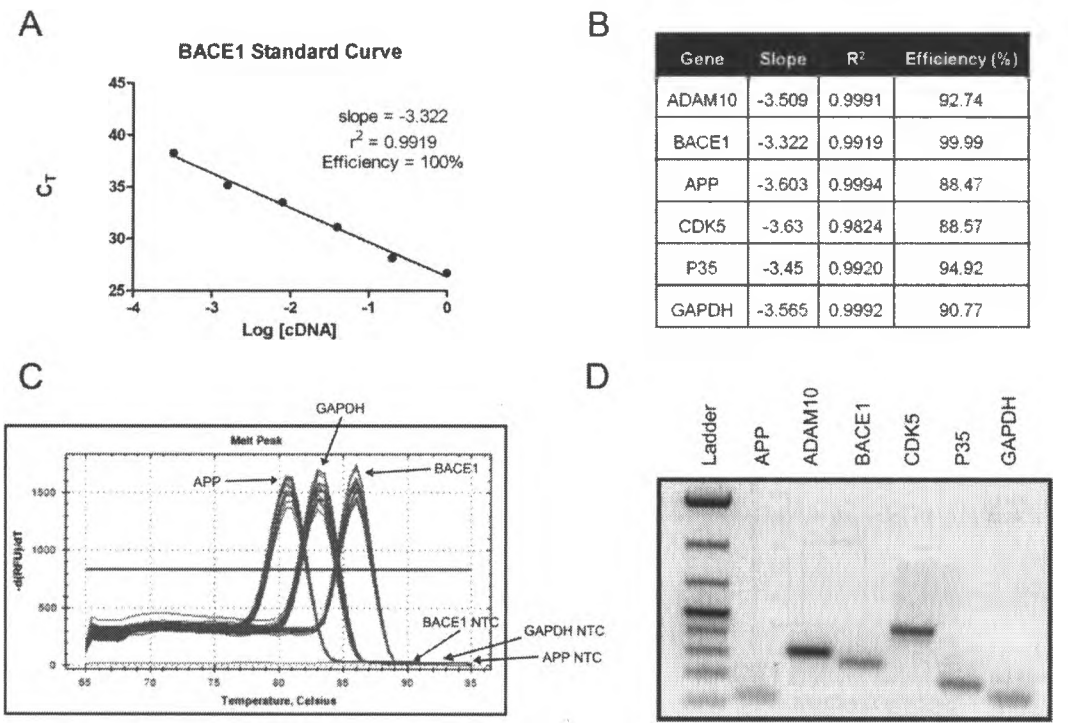

Gene	Slope	R^2	Efficiency (%)
ADAM10	-3.509	0.9991	92.74
BACE1	-3.322	0.9919	99.99
APP	-3.603	0.9994	88.47
CDK5	-3.63	0.9824	88.57
P35	-3.45	0.9920	94.92
GAPDH	-3.565	0.9992	90.77

Figure 3.7: Confirmation of quality of primers used for real-time PCR in primary neurons. The efficiency of amplification of target genes for primers used for real-time PCR experiments in primary neurons was determined by generating standard curves of serially diluted cDNA plotted against their Ct values. An efficiency between 90 and 110% was considered optimal when calculated according to the formula $[10^{(-1/slope)} - 1] \times 100$. A representative standard curve is given (Panel A) and the parameters of all primers used are summarized (Panel B). The amplification of single PCR products by each product was confirmed by performing melting curve analysis of each amplicon. An example of melting peaks for APP, BACE1, GAPDH as well as their no template controls (NTC) is shown (Panel C). Additionally, a single PCR product for each gene was confirmed by visualization of amplicons on a 1% agarose gel by ethidium bromide (Panel D).

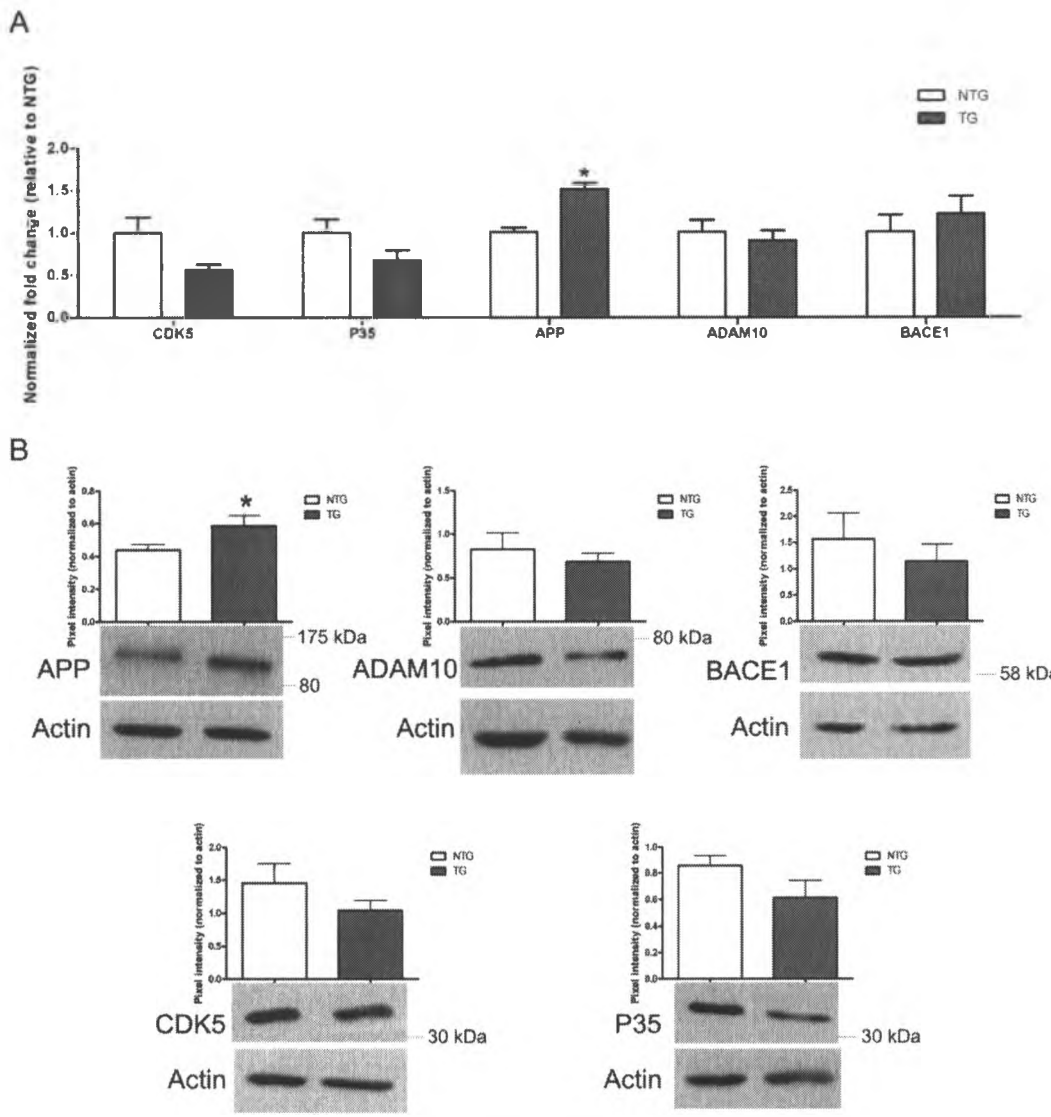

Figure 3.8: APP processing in cortical cultures from APP/PS1 mice. Endogenous levels of APP processing genes were examined at the level of mRNA (Panel A) by real-time PCR and protein (Panel B) by immunoblots in primary cortical cultures of APP/PS1 mice at 8 DIV. Immunoreactive bands were quantified and pixel intensity was normalized to actin levels; representative immunoblots are shown. Data are expressed as mean ± SEM of 5 independent experiments, * = $p < 0.05$.

3.7 mRNA and protein levels of APP processing genes are altered by expression of 82-ChAT

The functional significance of 82-ChAT is not well understood, nor is it clear what role this protein has being located within the nucleus of cholinergic neurons. Gill and colleagues observed previously that 82-ChAT is expressed endogenously in cholinergic neurons in human brain and spinal cord. An age-related shift in 82-ChAT from nuclei of neurons to the cytoplasm was observed, and this was exacerbated in cholinergic neurons in AD brain tissue (Gill et al 2007). The nuclear localization of this neurotransmitter-synthesizing enzyme has prompted studies to assess alternative functional roles potentially related to AD. In microarray studies, it was observed that the expression of 82-ChAT in IMR32 human neuroblastoma cells altered gene expression in a manner that favoured the non-amyloidogenic processing of APP (Gill et al, unpublished observation).

Based on these preliminary studies, we decided to explore how expressing 82-ChAT alters APP processing in SH-SY5Y human neuroblastoma cells and in primary cortical neurons prepared from APP/PS1 double transgenic mice. The mRNA and protein levels for APP, ADAM10, BACE1, CDK5 and P35 were analyzed.

3.7.1 SH-SY5Y cells

For SH-SY5Y cells, primers specific to the human genome were used to amplify each gene of interest by real-time PCR. Primer quality (Figure 3.9) was confirmed by calculating amplification efficiency and ensuring single amplicons

A

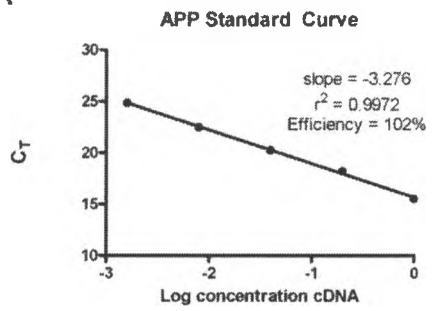

B

Gene	Slope	R^2	Efficiency (%)
ADAM10	-3.18	0.9907	106.28
BACE1	-3.61	0.9964	89.24
APP	-3.276	0.9972	101.95
CDK5	-3.101	0.9752	110.12
P35	-3.342	0.9855	99.17
GAPDH	-3.37	0.9609	98.03

C

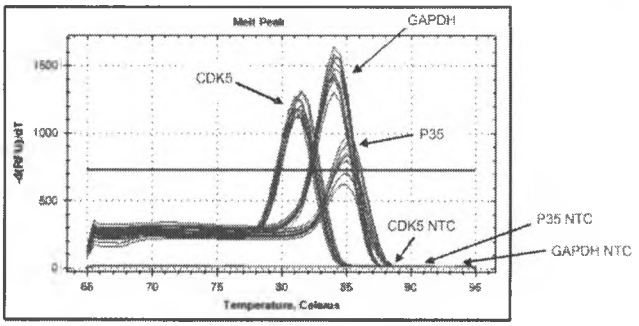

D

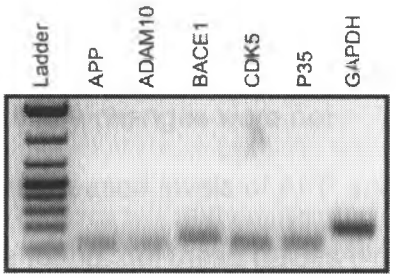

Figure 3.9: Confirmation of quality of primers used for real-time PCR in SH-SY5Y cells. The efficiency of amplification of target genes for primers used for real-time PCR experiments in SH-SY5Y cells was determined by generating standard curves of serially diluted cDNA plotted against their Ct values. Efficiency between 90 and 110% was considered optimal when calculated according to the formula $[10^{(-1/slope)} - 1] \times 100$. A representative standard curve is given (Panel A) and the parameters of all primers used are summarized (Panel B). The amplification of single PCR products by each product was confirmed by performing melting curve analysis of each amplicon. An example of melting peaks for CDK5, P35, and GAPDH as well as their no template controls (NTC) is shown (Panel C). Additionally, single PCR products for each gene were confirmed by visualization of amplicons on a 1% agarose gel by ethidium bromide (Panel D).

were produced as described previously for murine primers. mRNA levels were normalized to GAPDH and the fold-change was calculated for each 82-ChAT clone relative to empty vector expressing cells. Figure 3.10 summarizes the mRNA levels of each gene evaluated (Panel A), with representative immunoblots given in Panel B. A significant reduction in BACE1 (two-way ANOVA with Bonferroni post-hoc test, $p < 0.05$) mRNA levels was found in clone one (0.43 ± 0.08) relative to empty vector expressing cells (1.0 ± 0.25). This is consistent with the trends observed in protein levels of BACE1, but these changes were not seen in the second 82-ChAT clone. A trend towards increased levels of APP and ADAM10 and reduced levels of CDK5 and P35 were found, but these results did not reach the level of statistical significance.

3.7.2 Primary cortical neurons from APP/PS1 mice

For primary cortical cultures, murine primers were used to detect mRNA levels of each gene in cells transduced with 82-ChAT proteins relative to GFP-expressing controls. Figure 3.11 summarizes the fold-change mRNA levels found in the absence (Panel A) and presence (Panel B) of the transgenes. The most consistent changes found were elevated levels of ADAM10 with 82-ChAT expression, 1.19 ± 0.11 and 1.30 ± 0.18 fold-changes for NTG and TG mice, respectively. In NTG mice, a reduction in CDK5 (0.72 ± 0.08), P35 (0.64 ± 0.1), APP (0.86 ± 0.130), and BACE1 (0.83 ± 0.16) mRNA levels were found. In TG mice, CDK5 (1.27 ±0.32), P35 (1.41 ± 0.27), and APP (1.28 ± 0.13) were elevated. BACE1 mRNA levels in TG mice remained unchanged with 82-ChAT

expression (0.97 ± 0.37). These changes in mRNA levels did not reach the level of statistical significance when data was analyzed by two-way ANOVA with Bonferroni's post-hoc tests.

Levels of APP, ADAM10, BACE1, CDK5 and P35 proteins in cells transduced with 82-ChAT and GFP adenoviruses were also measured by immunoblots. Immunoreactive bands were quantified and normalized to actin band intensity. Results from 5 independent experiments are summarized in Figure 3.12 and representative immunoblots are given. No significant changes were found in NTG mice, with trends towards an increase in APP, ADAM10 and P35 and reduction in BACE1 levels. Statistically significant changes were found in TG mice expressing 82-ChAT as compared to GFP when normalized pixel intensity was analyzed by two-way ANOVA with Bonferroni post-hoc tests. BACE1 levels were significantly reduced (0.99 ± 0.24 versus 0.49 ± 0.13 for GFP and 82-ChAT, respectively) while CDK5 (0.90 ± 0.06 versus 1.47 ± 0.12 for GFP and 82-ChAT, respectively) and P35 (0.83 ± 0.12 versus 1.37 ± 0.07 for GFP and 82-ChAT, respectively) were significantly elevated.

Overall, 82-ChAT expression favoured either elevated or unchanged levels of APP and ADAM10 and decreased or unchanged levels of BACE1 in both SH-SY5Y cells and in primary cortical neurons. Changes in CDK5 and P35 were inconsistent. A reduction was found in SH-SY5Y cells and mRNA in NTG mice. The opposite trend was found in mRNA levels of TG mice that translated to a significant increase in overall protein expression levels.

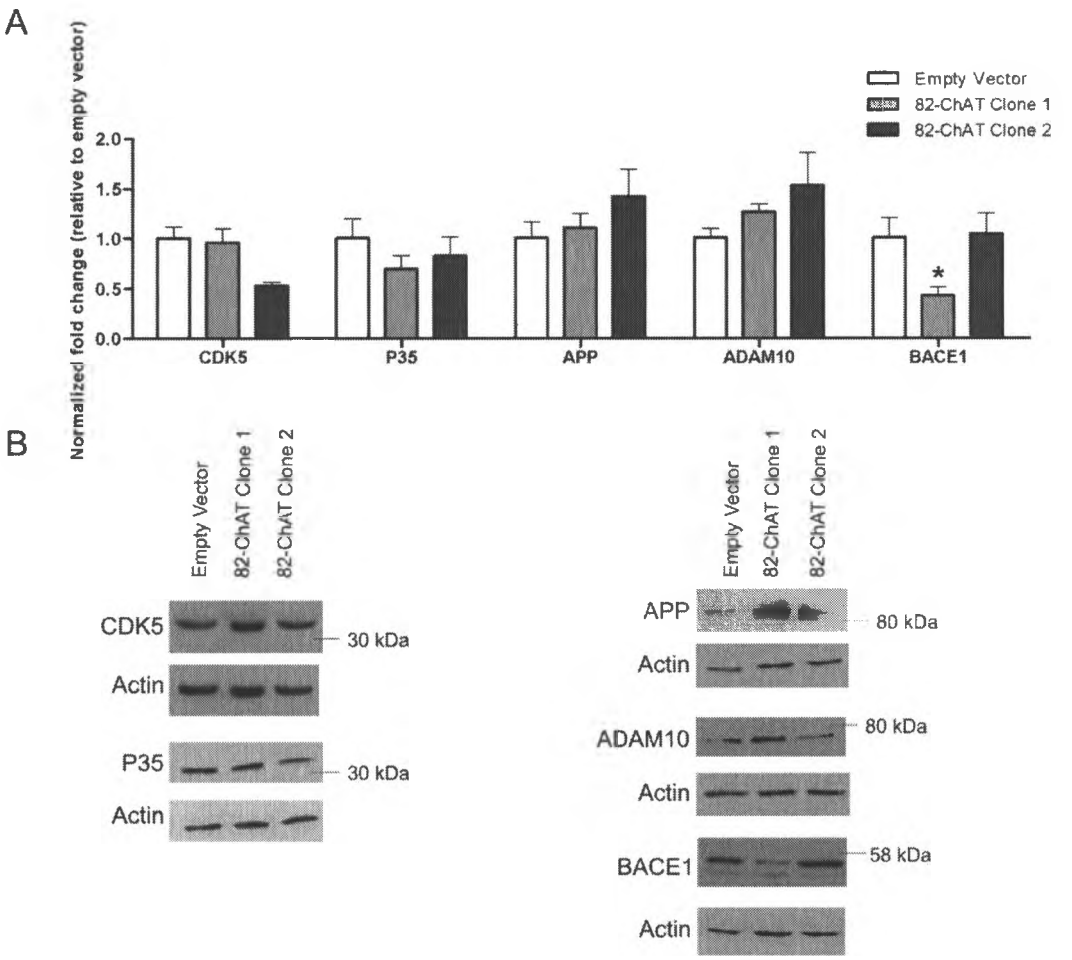

Figure 3.10: APP processing is altered in SH-SY5Y cells that stably express 82-ChAT. Endogenous levels of proteins involved in APP processing were examined at the level of mRNA (Panel A) by real-time PCR and protein (Panel B) by immunoblots in SH-SY5Y cells which over-express 82-ChAT. A significant reduction in BACE1 was observed, although changes were inconsistent between two 82-ChAT clones. For real-time PCR, data are expressed as ± SEM of 5 independent experiments, * = $p < 0.05$.

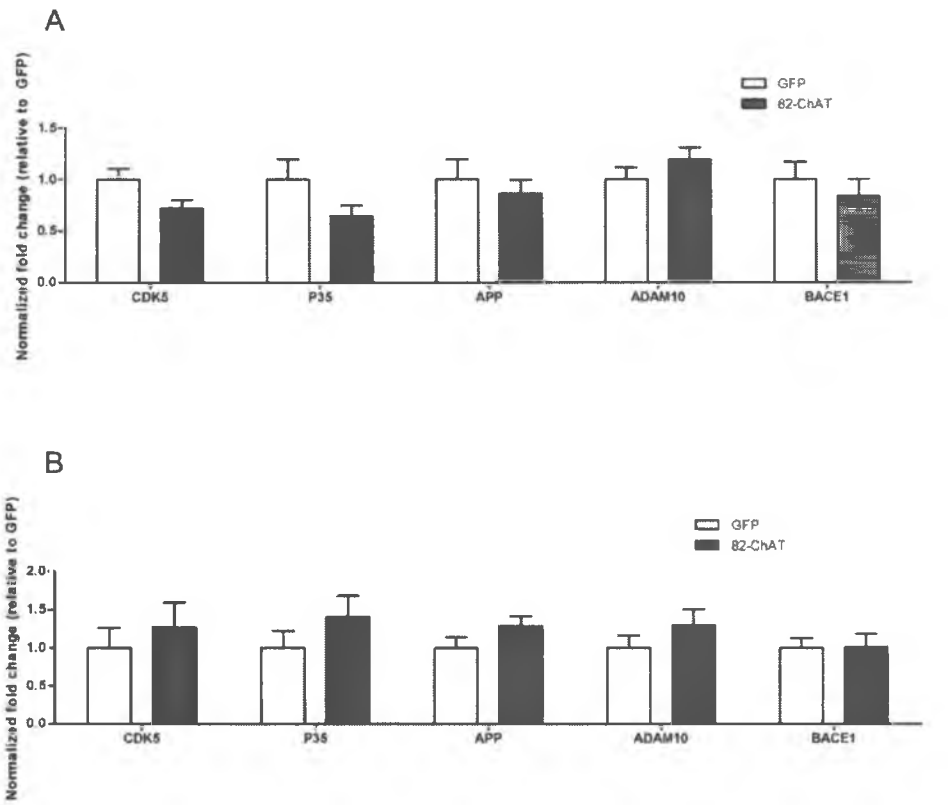

Figure 3.11: mRNA levels of APP processing proteins in cortical neurons that express 82-ChAT. mRNA levels of APP, ADAM10, BACE1, CDK5 and P35 were evaluated in 8 DIV primary cultures of APP/PS1 mice in the absence (Panel A) and presence (Panel B) of transgenes by real-time PCR. All data is expressed as mean ± SEM of 5 independent experiments.

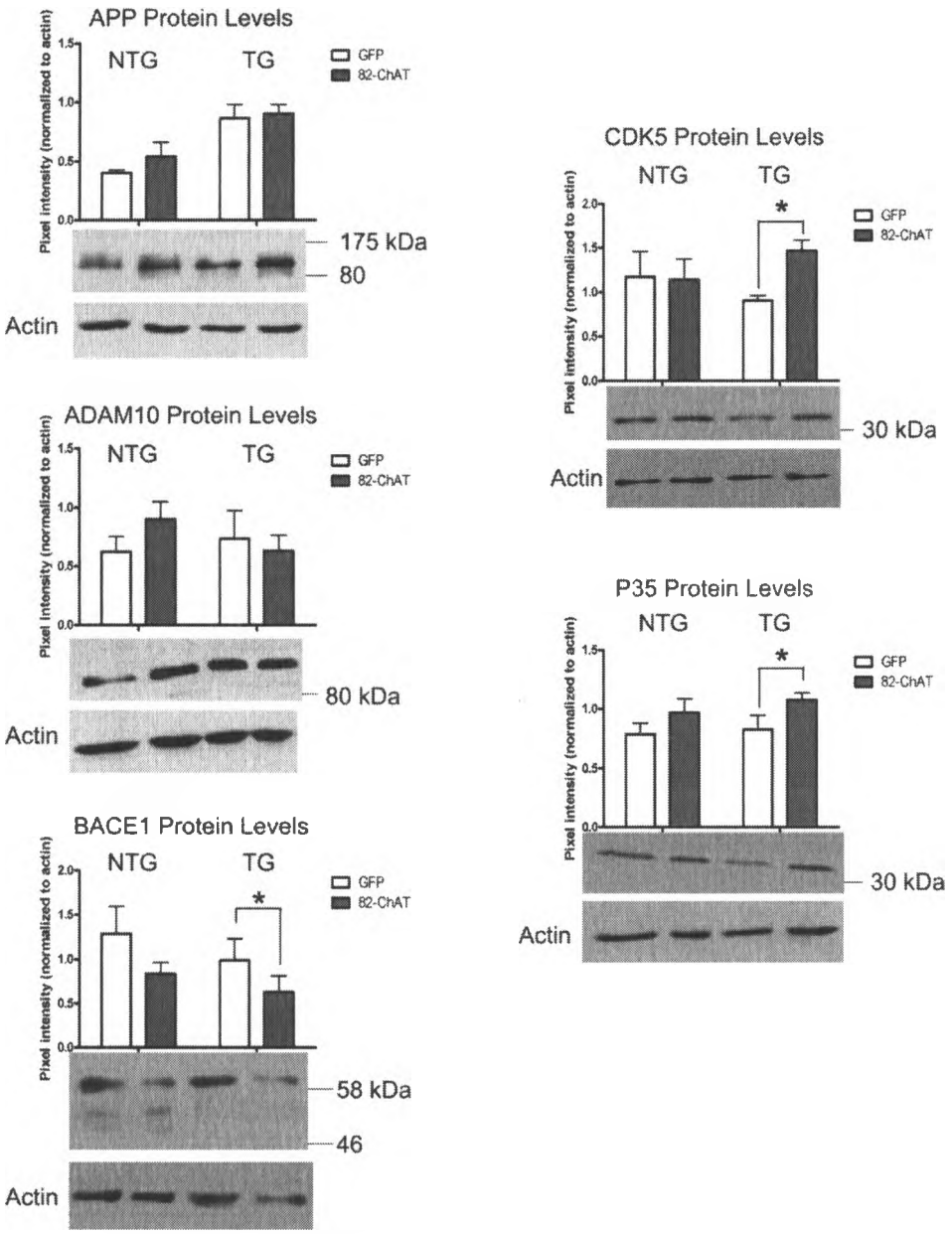

Figure 3.12: APP processing is altered at the protein level in cortical neurons that express 82-ChAT. Protein levels of APP, ADAM10, BACE1, CDK5 and P35 were evaluated in 8 DIV primary cultures of APP/PS1 mice by immunoblots; representative blots are given. Immunoreactive bands were quantified and pixel intensity was normalized to actin levels. All data are expressed as mean ± of SEM of a minimum of 5 independent experiments, * = $p < 0.05$.

3.8 Human $A\beta_{1-42}$ release from APP/PS1 cultures is reduced by 82-ChAT expression

The effect of 82-ChAT expression on $A\beta_{1-42}$ levels released into the media of cortical neuron cultures prepared from embryonic APP/PS1 double transgenic mice was also measured at 8 DIV by ELISA. $A\beta_{1-42}$ levels were normalized to total protein content of the cell lysates. Results from 5 independent experiments are summarized in Figure 3.13. Significantly less $A\beta_{1-42}$ was released from cells transduced to express 82-ChAT [0.8466 (pg/ml)/μg total protein] compared to GFP [1.046 (pg/ml)/μg total protein] as a control when analyzed using a paired Student's *t*-test ($p < 0.05$). This was equivalent to approximately a 20% reduction in $A\beta_{1-42}$ levels.

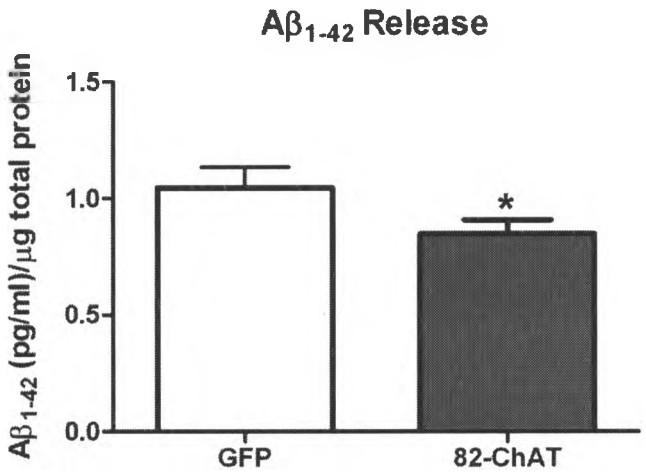

Figure 3.13: Expression of 82-ChAT decreases $A\beta_{1-42}$ released from cortical cultures of APP/PS1 mice. ELISA was used to measure soluble $A\beta_{1-42}$ levels in 8 DIV primary cortical cultures of APP/PS1 mice which express 82-ChAT. $A\beta_{1-42}$ release was normalized to total protein concentration in cell lysates. A significant reduction in soluble $A\beta_{1-42}$ levels was found in cells expressing 82-ChAT. Data are expressed as mean ± SEM of 5 independent experiments, * = $p < 0.05$.

CHAPTER FOUR: DISCUSSION

4.1 Conclusions

Specific Aim 1

1. Significant levels of $A\beta_{1-42}$ are released from primary neuron cultures prepared from TG APP/PS1 mice at 8 and 11 DIV.
2. Human Aβ/APP is found in cytoplasm and cell processes of neurons cultured from cerebral cortex of TG mice.
3. The elevation in $A\beta_{1-42}$ in TG mice is not due to changes in levels of APP processing enzymes, but instead due to increased levels of APP.

Specific Aim 2

1. Introduction of 82-ChAT cDNA into primary cortical neurons by an adenoviral delivery system leads to production of a functional protein that is predominantly localized to cell nuclei.
2. In human neural cells, stable expression of 82-ChAT results in a significant reduction in BACE1 levels. Trends towards decreased CDK5 and P35 levels and increased ADAM10 and APP levels are also observed.
3. Expression of 82-ChAT reduces the amount of $A\beta_{1-42}$ released into culture media from cortical neuron cultures from APP/PS1 TG mice at 8 DIV.
4. 82-ChAT expression did not significantly alter mRNA levels of APP processing proteins. A significant reduction in BACE1 protein levels in TG mice indicates 82-ChAT may alter proteins that are involved in post-translational modification and trafficking of BACE1.

4.2 Contribution to current knowledge of AD and 82-ChAT

The aim of these studies was to enhance our understanding of the function of 82-ChAT protein, particularly in relation to APP and Aβ metabolism. ChAT is encoded by a single gene, but alternative splicing results in multiple mRNA species. All ChAT mRNAs translate into the 69-kDa ChAT protein; however, the M-transcript in primates also encodes an 82-kDa isoform of ChAT (Misawa et al 1997). 82-ChAT differs from 69-ChAT by a 118 residue amino terminal extension. A functional NLS is found in this region of the protein directs 82-ChAT to the nucleus while 69-ChAT is found largely in the cytoplasm (Resendes et al 1999; Gill et al 2003). The functional significance of the different subcellular distribution of ChAT proteins is unknown. Gill and colleagues (2007) found that with increasing age, 82-ChAT protein is lost from the nucleus and this is accelerated in mild cognitive impairment and AD. These findings prompted microarray studies which found that 82-ChAT alters expression of several tramscripts in a direction that favours the non-amyloidogenic processing of APP (Gill et al, unpublished observation). This work points towards a protective role for the 82-ChAT protein in relation to the Aβ pathology of AD. The studies described in this thesis support these findings and provide a better understanding of 82-ChAT function.

4.2.1 Characterization of Aβ pathology in APP/PS1 primary neuron cultures

A goal of the present studies was to determine if expression of human 82-ChAT alters production of Aβ by primary neuronal cultures prepared from brain of

a murine model with significant Aβ deposition. The APP/PS1 double transgenic mouse is a commonly used model of AD because of the onset of Aβ pathology from as early as 4 months of age (Garcia-alloza et al 2006, Machova et al 2008). However, primary embryonic neuron cultures created from this transgenic mouse model have not been studied, nor have they been characterized for their ability to generate Aβ. Initial investigations using this culture system involved determining if sufficient Aβ is released from embryonic neurons for the purposes of these studies. We used an ELISA specific for detection of human $A\beta_{1-42}$ to measure its levels in conditioned media from cortical neurons after various times in culture. Human $A\beta_{1-42}$ proteins could only be detected in the presence of the transgenes with significant levels of this peptide observed at 8 and 11 DIV (Figure 3.5). At 8 DIV, media samples were concentrated and analyzed by SDS-PAGE in order to determine if there is oligomerization of Aβ peptides and confirm the ELISA results. Unfortunately, we were unable to detect these peptides with the experimental methods used. This was technically difficult and likely confounded by aggregation of Aβ proteins occurring during concentration to reduce the volume of the culture media or during preparation of the samples. The increased production of the more hydrophopic form of Aβ, $A\beta_{1-42}$, from these neurons increased the difficulty of detecting these peptides by immunoblots.

Endogenous proteins involved in the processing of APP were examined at both the level of mRNA and protein (Figure 3.8). Primers specific to the murine genome were used to determine mRNA levels while antibodies that recognize both human and murine proteins were used for immunoblots. APP levels were

found to be significantly elevated in TG mice compared to NTG littermate controls. This was expected at the protein level because this mouse model was generated by incorporating an additional copy of the human APP gene carrying the Swedish mutation (Jankowsky et al 2004). AICD, which is released following γ-secretase cleavage of APP, has been implicated to play a role in altering gene transcription. By forming a complex with the nuclear adaptor protein Fe65 and the histone acetyltransferase Tip60, AICD is able to increase transcription of genes such as APP (Cao and Sudhof 2001; von Rotz 2004). This may account for some of the changes seen in mouse APP mRNA levels in the neuron cultures we prepared from TG mice. We observed that ADAM10 levels and BACE1 protein levels were slightly decreased while BACE1 mRNA levels were slightly elevated in TG mice neuron cultures. The significant Aβ levels we measured in these TG mice could not be attributed to changes in levels of secretases that cleave APP. Instead, the increased APP proteins are cleaved more readily by the BACE1 proteins that are already made in the cell.

CDK5 and its regulatory protein P35 have been implicated for their role in AD by directly phosohorylating tau proteins and increasing BACE1 mRNA levels to mediate Aβ production (Iijima et al 2000; Town et al 2002; Liu et al 2003; Wen et al 2008). In this study, we examined endogenous levels of CDK5 and P35 to determine if these proteins could contribute to the Aβ production that was observed in primary neuron cultures of TG mice. A decrease in mRNA and protein levels was found for CDK5 and P35, which was the opposite of what we expected initially. However, over-expression of the Swedish mutant form of APP

has been shown to reduce the stress-induced activity of CDK5. APP knock-out mice also show increased levels of CDK5 activity, which is associated with increased levels of tau phosphorylation. This indicates that APP may actually prevent tau phosphorylation by modulating CDK5 activity (Han et al 2005). This may account for the decrease in CDK5 and P35 observed in the cortical neuron cultures of TG mice. Additionally, the conversion of P35 to P25 was not observed by immunoblots in TG mice cortical cultures (data not shown). This indicates that CDK5 did not play a role in modulating Aβ production in this cell model.

4.2.2 Contribution to current knowledge of 82-ChAT

The differential subcellular distribution of 69- and 82-ChAT indicates that these proteins may have different biological functions within the different cellular compartments. The ability of 82-ChAT to synthesize ACh *in vivo* has not been demonstrated. The presence of muscarinic AChRs on the nuclear envelope has been reported, but the orientation of these receptors is not known (Lind and Cavanagh 1993, 1995). 82-ChAT may instead modulate cellular processes that are alternative to the ACh-synthesizing function mediated by 69-ChAT proteins.

A significant result from the present studies is that ChAT expression in neuronal cells can alter APP metabolism. Cholinergic neurons in the brain contain high levels of APP (Harkany et al 2002) and have been shown to impact APP processing pathways in their target cells. Activation of muscarinic AChRs results in increased levels of α-secretase cleavage products of APP such as sAPPα (Robner et al 1998; Davis et al 2010). However, the regulation of APP

processing within cholinergic neurons has not received much attention. In the present study, we show that 82-ChAT protein expression can influence APP metabolism, with the greatest effects on BACE1 levels. A significant reduction in BACE1 levels in 82-ChAT expressing SH-SY5Y cells was found with trends towards reduced levels of CDK5 and P35 and increased APP and ADAM10 (Figure 3.10). In primary cultures (Figures 3.11 and 3.12), trends towards reduced levels of BACE1 and elevated ADAM10 levels were found, with changes in BACE1 protein levels in TG mice reaching statistical significance. Although the changes in mRNA levels did not all reach the level of statistical significance, the functional outcome of these trends favours non-amyloidogenic processing. These results translated to a 20% reduction of human $A\beta_{1-42}$ released from cortical neurons cultured from TG mice expressing 82-ChAT compared to GFP-expressing control cultures (Figure 3.13).

Since only a subpopulation of the virus-transduced cultured cortical neurons expressed the 82-ChAT protein, the effect may not have been sufficient to reveal significant effects on secretase mRNA levels. Also, 82-ChAT may have a more extensive effect on APP processing, altering mRNA levels of proteins involved in its post-translational regulation and modification of secretases. This was observed with the significant reduction in the protein level of BACE1 in primary neuron cultures by 82-ChAT. BACE1 is initially produced as an immature pro-BACE1 in the endoplasmic reticulum and must undergo gylcosylation and processing by a furin-like convertase as it travels through the Golgi (Haniu et al 2000; Vassar 2004). Phosphorylation of BACE1 on Ser-498 and a carboxyl-

terminus dileucine motif regulate its recycling between the cell surface and endosomal and/or lysosomal compartments (Huse et al 2000; Walter et al 2001; Koh et al 2005). The ubiquitin-proteasome pathway has also been implicated in the degradation of BACE1. Treatment of SH-SY5Y cells with lactacystin, a selective inhibitor of the 20S proteasome, results in significant elevation of endogenous BACE1 protein levels (Qing et al 2004). One possibility is that 82-ChAT alters transcript levels of proteins involved in the regulation of BACE1 trafficking, targeting BACE1 protein to a degradation pathway. Furthermore, the efficiency of BACE1 translation is elevated following energy depravation through phosphorylation of the translation initiation factor eIF2α (O'Connor et al 2008). In post-mortem human AD brain samples, elevated levels of phosphorylated eIF2α levels positively correlate to increased BACE1 and amyloid production. 82-ChAT may decrease BACE1 protein levels by attenuating BACE1 translation.

The elevation in protein levels of CDK5 and P35 in TG mice with 82-ChAT expression was unexpected because this would result in increased production of Aβ. The baseline reduction in CDK5 and P35 mRNA levels in TG mice indicates that CDK5 does not contribute to the Aβ production in these mice. CDK5 also has important functions in the brain, playing a role in axonal extension (Connell-Crowley et al 2000; Nikolic et al 1996), associative learning (Fischer et al 2002), and synaptic vesicle endocytosis by phosphorylating proteins such as dynamin 1 (Tan et al 2003). Increasing levels of CDK5 and P35 may be important for regulation of these processes by 82-ChAT.

Aβ peptides have been shown to reduce cholinergic transmission and decrease ChAT activity (Zambrzycka et al 2002; Machova et al 2008, 2010). By decreasing Aβ production, 82-ChAT may counteract these detrimental effects on cholinergic neurons and facilitate communication within the brain. Also, favouring non-amyloidogenic processing of APP may lead to increased levels of sAPPα which has neurotrophic properties (Thornton et al 2006; Gakhar-Koppole et al 2008). Based on these studies, increasing activity or levels of 82-ChAT protein may be a beneficial target for future therapies aimed at reducing Aβ production.

The cognitive deficits of AD correlate best with a decline in ChAT activity in the forebrain, and significant cell loss in this brain area is observed post-mortem. However, studies indicate that these cholinergic pathologies do not develop early in AD but are present later in the disease progression (Davis et al 1999; Tiraboschi et al 2002). In contrast, ChAT levels may be elevated or unchanged at early stages of AD (Davis et al 1999; Gilmor et al 1999; DeKosky et al 2002). Gill and colleagues (2007) found increased staining for 82-ChAT in the clastrum from subjects with mild cognitive impairment and an absence of staining in advanced AD. This phenomenon is also evident in some mouse models of AD. For example, ChAT activity is elevated in the hippocampus and other neocortical areas of 10 month old Ts65Dn mice (Contestabile et al 2006).

APP/PS1 transgenic mice have cholinergic neuritic swellings in the cortex and hippocampus in response to increases in Aβ load (Hernandez et al 2001; Perez et al 2007). Additionally, activation of both nicotinic (Hernandez et al 2010) and muscarinic (Davis et al 2010) AChRs has been implicated in reducing Aβ

deposition in mouse models of AD by altering APP cleavage products. Taken together, this suggests that there may be a compensatory mechanism in the cholinergic system to resist the pathology of AD. By shifting the processing of APP to the non-amyloidogenic pathway, cholinergic neurons may reduce Aβ production and increase sAPPα levels in target cells. In the present study, this was observed by decreased BACE1 which translated to reduced $A\beta_{1-42}$ production overall. Perhaps in the brain of individuals with ensuing mild cognitive impairment or AD, a loss of 82-ChAT protein from the nucleus over time may diminish the ability of cholinergic neurons to fight Aβ pathology and make them more susceptible to neurodegeneration.

The mechanisms by which 82-ChAT may regulate gene expression to alter mRNA levels are unknown. It has not been determined if 82-ChAT is involved in the direct interaction with DNA; however, the presence of surface accessible basic residues in ChAT proteins may mediate this association (Cai et al 2004; Kim et al 2006). Alternatively, acetylation is a major post-translational event that is involved in the modification of histones, transcription factors and other regulatory proteins in the nucleus. 82-ChAT may be involved in the acetylation of lysine residues in histones or other proteins to control gene expression. However, 82-ChAT is an *O*-acetyltransferase and has not been shown to perform the *N*-acetylation reaction that would be required for modification of proteins. The structure of ChAT consists of a solvent accessible tunnel at the interface of two large globular domains. Substrates enter from opposite ends of the tunnel to access the catalytic site, and a small

conformational change in ChAT occurs upon binding of acetyl-CoA (Kim et al 2006). Thus, the narrow tunnel is best suited for binding to small molecules such as acetyl-CoA and choline or choline analogues, and the likelihood that proteins could gain access to the catalytic site of ChAT for acetylation is low.

On the other hand, post-translational modifications may be important for modifying the conformation of ChAT proteins, thus altering the ability of 82-ChAT to acetylate substrates or interact with other regulatory proteins. Phosphorylation is the most abundant post-translational regulatory mechanism in cells. It plays a role in processes such as enzyme activation or inactivation, protein degradation via the ubiqutin/proteasome pathway, and facilitation of protein-protein interactions. Phosphorylation by protein kinase C (PKC) has been shown to increase the catalytic activity of both 69- and 82-ChAT proteins (Dobransky et al 2000, 2001) and can alter the binding of 69-ChAT to subcellular membranes (Dobransky et al 2001). The addition of toxic insults can also alter the phosphorylation of proteins. For example, genotoxic stresses induce phosphorylation of p53 which are important for stabilization of the protein and allow it to exert its tumor suppressive functions (Appella and Anderson 2001). Also, treatment of neuroblastoma cells with $A\beta_{1-42}$ results in phosphorylation of 69-ChAT at serine-440 by PKC and transiently activates ChAT. This is followed by phosphorylation at threonine-456 by Ca^{2+}/calmodulin-dependent protein kinase II which results in decreased ChAT activity and is associated with an interaction with valosin-containing protein (VCP; Dobransky et al 2003). VCP is an AAA^{+}-ATPase involved in multiple cellular functions, including protein

degradation. The significance of the interaction of 69-ChAT and VCP is not understood, but may be important for ChAT protein turnover and availability to synthesize ACh. Also, the interaction between 82-ChAT and VCP or any other proteins have not yet been determined. Phosphorylation may be an important event allowing 82-ChAT to interact with proteins to alter gene transcription or increase its enzymatic activity to maintain cholinergic neurotransmission. In early stages of AD, a toxic interstitial environment in the brain and within neurons may facilitate the phosphorylation of 82-ChAT, thus providing some resistance to the approaching pathology.

Alternatively, 82-ChAT may function to synthesize ACh as both choline and acetyl CoA are found in the nucleus. The purpose for having ACh in the nucleus is unknown. ACh normally acts to activate pre- and post-synaptic nicotinic and muscarinic AChRs which elicit further cellular events via an influx of Ca^{2+} ions or G-protein signalling. Non-neuronal ChAT proteins are involved in the synthesis of ACh and perform a variety of functions. The effects of ACh in these cells are largely mediated by altering the intracellular Ca^{2+} ion levels. For example, ACh activates muscarinic AChRs in granulosa cells isolated from human follicles and results in elevated Ca^{2+} levels that alter transcription factors important for cell differentiation (Mayerhofer and Kunz 2005). Activation of nicotinic AChRs in human mesenchymal stem cells can increase Ca^{2+} influx into cells and induce spontaneous cell migration (Schraufstatter et al 2010). The nucleus is surrounded by a lipid bilayer called the nuclear envelope. Nuclear pore complexes (NPCs) embedded in the membrane regulate the transport of

molecules in and out of the nucleus (Lim et al 2008). Ca^{2+} ions sequestered in the nuclear membrane have been shown to influence NPC conformation (Erickson et al 2006). Additionally, muscarinic AChRs (Lind and Cavanagh 1993, 1995), angiotensin receptors (Eggena et al 1993), ryanodine receptors (George et al 2007) and inositol triphosphate receptors (Erickson et al 2006) have been found on the nuclear envelope. It may be possible that 82-ChAT synthesizes ACh to interact with these receptors and modulate Ca^{2+} levels in the nucleus. Here, Ca^{2+} can alter many processes including gene expression (Dolmetsch et al 1998). This may also be an indirect mechanism whereby the AChRs are able to reduce Aβ deposition.

The focus of the present study was to assess the ability of 82-ChAT proteins to modulate the Aβ production that has been associated with AD pathology. However, there have been many other cellular processes implicated to play a role in the pathogenesis of AD. These include neuroinflammation, hyperphosphorylation of tau and neurofibrillary tangle formation, aberrant cell cycle activation, and oxidative stress. By altering gene transcription either directly or indirectly, the effects of 82-ChAT may be widespread (summarized in Figure 4.1). Further studies could focus on how 82-ChAT can affect these other disease mechanisms and how these changes may interact.

4.3 Limitations and suggestions for future studies

Possible Limitations

The major limitation to this study was the spread of genotypes of embryos from each litter. In this study, male mice that were hemizygous for transgenes (TG) were mated with wild-type female mice [i.e. they do not express the transgenes]. According to Mendelian genetics, the resulting litters should have equal numbers of NTG and TG embryos. However, this rule is only true when measured over relatively large populations. As a result, most of the mouse litters we used had an uneven distribution of genotypes with a majority of pups being either the NTG or TG. Because dissociated brain neurons were plated as cell cultures before the results of the genotyping could be obtained and as re-plating of primary neuronal cultures is not possible, this limited the availability of cultured cells for each comparison within each experiment.

Another limitation was that human neural cell lines have not been identified that express 82-ChAT endogenously. Thus, we were only able to study experimental models that were engineered using recombinant DNA technologies to stably over-express 82-ChAT and did not have the opportunity to use models where 82-ChAT could be knocked-down. Additionally, the 82-kDa isoform of ChAT is expressed only in primates (Misawa et al 1997). For studies involving murine primary neuron cultures, over-expression of 82-ChAT was accomplished using an adenoviral gene delivery system that yielded only approximately 50% transduction efficiency. The expression of 82-ChAT under these conditions was limited by the sensitivity of cells to toxicity of the viral gene delivery system. Cells

were susceptible to toxicity when exposed to higher concentrations of the adenoviruses and this was increased as they became more differentiated with time in culture. A greater effect of 82-ChAT on the measures made may have been observed in primary neuron cultures if transduction efficiency could have been improved.

Future Studies

Significant information was obtained in this thesis about the APP/PS1 mouse model of AD, as well as 82-ChAT proteins. However, these studies focused on Aβ pathology and APP processing. Future studies could explore other aspects of AD pathology in primary cultures of this mouse model as well as how they may be altered by 82-ChAT. For example, neuroinflammatory or oxidative stress pathways could be studied. Furthermore, generation of a transgenic knock-in model of 82-ChAT would allow further characterization of the functional significance of this protein. These mice could also be crossed with the APP/PS1 model to determine the effects of 82-ChAT on Aβ production and other pathologies at different times in the lifespan of the mouse.

Future studies may also be aimed at better understanding of the mechanisms by which 82-ChAT may function in the nucleus. This includes assays to determine if 82-ChAT can interact directly with DNA or acetylate histones. Also, protein interaction screens can be used to uncover novel proteins that interact with 82-ChAT. This may include transcription factors or regulatory proteins that are important for 82-ChAT to function in the nucleus. Finally, the

role of post-translational modifications such as phosphorylation or SUMOylation should be examined for their role in altering 82-ChAT activity or function.

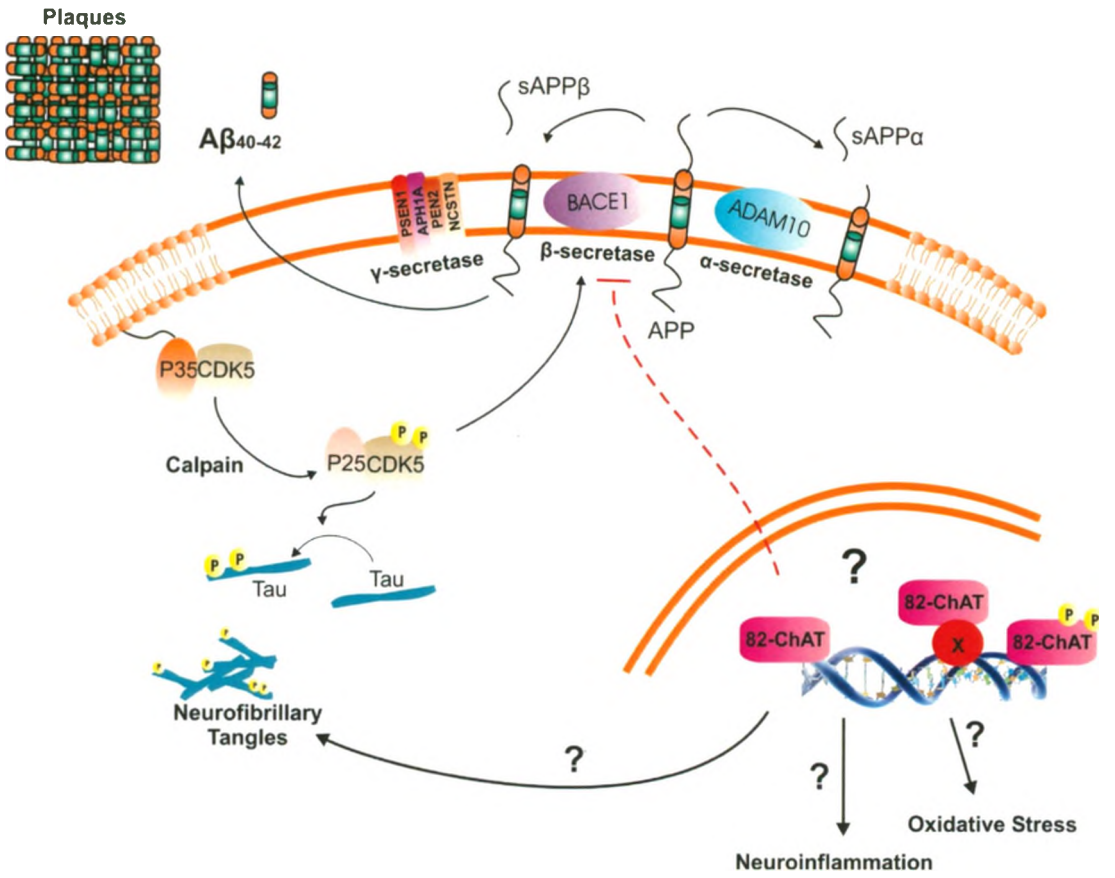

Figure 4.1: A neuroprotective role of 82-ChAT in the brain. 82-ChAT is found in nuclei of cholinergic neurons in primates; however, the function of this protein has not yet been elucidated. I found that expression of 82-ChAT decreases BACE1 levels, thereby decreasing Aβ production. By binding to DNA or other mechanisms, 82-ChAT may have a protective role in the diseased brain, influencing various aspects of AD pathology.

CHAPTER FIVE: REFERENCES

Alvarez A., Munoz JP., and Maccioni RB (2001). A Cdk5–p35 stable complex is involved in the β-amyloid-induced deregulation of Cdk5 activity in hippocampal neurons. *Exp. Cell. Res.* **264,** 266–274.

Amos LA (2004). Microtubule structure and its stabilisation. *Org. Biomol. Chem.* **2**, 2153-2160.

Appella E., and Anderson CW (2001). Post-translational modifications and activation of p53 by genotoxic stresses. *Eur. J. Biochem.* **268**, 2764-2772.

Aubert I., Cecyre D., Gauthier S., and Quirion R (1996). Comparative ontogenic profile of cholinergic markers, including nicotinic and muscarinic receptors in the rat brain. *J. Comp. Neurol.* **369**, 31-55.

Ballatore C., Lee VM., and Trojanowski JQ (2007). Tau-mediated neurodegeneration in Alzheimer's disease and related disorders. *Nat Rev Neurosci* **8**, 663–672.

Bird TD., Stranahan S., Sumi SM., and Raskind M (1983). Alzheimer's disease: choline acetyltransferase activity in brain tissue from clinical and pathological subgroups. *Ann. Neurol.* **14**, 284–293.

Bondi MW., Salmon DP., Monsch AU., Galasko D., Butters N., Klauber MR., Thal LJ., and Saitoh T (1995). Episodic memory changes are associated with the ApoE-epsilon 4 allele in non-demented older adults. *Neurol.* **45**, 2203–2206.

Bondi MW., Salmon DP., Galasko D., Thomas RG., and Thal LJ (1999). Neuropsychological function and Apolipoprotein E genotype in the preclinical detection of Alzheimer's disease. *Psych. Aging* **14**, 295–303.

Braak H., and Braak E (1991). Neuropathological staging of Alzheimer-related changes. *Acta Neuropathol.* **82,** 259.

Cai Y., Cronin CN., Engel AG., Ohno K., Hersh LB., and Rodgers DW (2004). Choline acetyltransferase structure reveals distribution of mutations that cause motor disorders. *EMBO J.* **23**, 2047-2058.

Cao X., and Sudhof TC (2001). A transcriptively active complex of APP with Fe65 and histone acetyltransferase Tip60. *Science*. **293**, 115-120.

Carbini L A., and Hersh LB (1993). Functional analysis of conserved histidines in choline acetyltransferase by site-directed mutagenesis, *J. Neurochem.* **61**, 247-253.

Chen HS., and Lipton SA (1997). Mechanism of memantine block of NMDA activated channels in rat retinal ganglion cells. *J. Physiol.* **499**, 27–49.

Citron M., Oltersdorf T., Haass C., McConlogue L., Hung AY., Seubert P., Vigo-Pelfrey C., Lieberburg I., and Selkoe DJ (1992). Mutation of the β-amyloid precursor protein in familial Alzheimer's disease increases β-protein production. *Nature* **360**, 672-674.

Collier B., and Katz HS (1974). Acetylcholine synthesis from recaptured choline by a sympathetic ganglion. *J. Physiol.* **238**, 639-655.

Connell-Crowley L., Le Gall M., Vo DJ., and Giniger E (2000). The cyclin-dependent kinase Cdk5 controls multiple aspects of axon patterning in vivo. *Curr. Biol.* **10**, 599-602.

Contestabile A., Fila T., Bartesaghi R., Contestabile A., and Ciani E (2006). Choline acetyltransferase activity at different ages in brain of Ts65Dn mice, an animal model for Down's syndrome and related neurodegenerative diseases. *J. Neurochem.* **97**, 515-526.

Cooke LJ., and Rylett RJ (1997). Inhibitors of serinerthreonine phosphatases increase membrane-bound choline acetyltransferase activity and enhance acetylcholine synthesis. *Brain Res.* **751**, 232-238.

Cozzari C., and Hartman BK (1980). Preparation of antibodies specific to choline acetyltransferase from bovine caudate nucleus and immunohistochemical localization of the enzyme. *Proc. Natl. Acad. Sci. USA.* **77**, 7453-7457.

Cruz JC., Kim D., Moy LY., Dobbin MM., Sun X., Bronson RT., and Tsai LH (2006). p25/cyclin-dependent kinase 5 induces production and intraneuronal accumulation of amyloid beta *in vivo*. *J. Neurosci.***26,** 10536-10541.

Davies P., and Maloney AJ (1976). Selective loss of central cholinergic neurons in Alzheimer's disease. *Lancet.* **2**, 1403.

Davis AA., Fritz JJ., Wess J., Lah JJ., and Levey AI (2010). Deletion of M1 muscarinic acetylcholine receptors increases amyloid pathology in vitro and in vivo. *J. Neurosci.* **30**, 4190-4196.

Davis KL., Mohs RC., Marin D., Purohit DP., Perl DP., Lantz M., Austin G., and Haroutunian V (1999). Cholinergic markers in elderly patients with early signs of Alzheimer disease. *JAMA*. **281**, 1401-1406.

DeKosky ST., Ikonomovic MD., Styren SD., Beckett L., Wisniewski S., Bennett DA., Cochran EJ., Kordower JH., and Mufson EJ (2002). Upregulation of choline acetyltransferase activity in hippocampus and frontal cortex of elderly subjects with mild cognitive impairment. *Ann. Neurol.* **51**, 145-155.

Dobransky T., Davis WL., Xiao GH., and Rylett RJ (2000). Expression, purification and characterization of recombinant human choline acetyltransferase: phosphorylation of the enzyme regulates catalytic activity. *Biochem. J.* **349**, 141-151.

Dobransky T., Davis WL., and Rylett RJ (2001). Functional characterization of phosphorylation of 69-kDa human choline acetyltransferase at serine 440 by protein kinase C. *J. Biol. Chem.* **276**, 22244-22250.

Dobransky T., Brewer D., Lajoie G., and Rylett RJ (2003). Phosphorylation of 69-kDa choline acetyltransferase at threonine 456 in response to amyloid-beta peptide 1-42. *J. Biol. Chem.* **278**, 5883-5893.

Dobransky T., Doherty-Kirby A., Kim AR., Brewer D., Lajoie G., and Rylett RJ (2004). Protein kinase-C isoforms differentially phosphorylate human choline acetyltransferase regulating its catalytic activity. *J. Biol. Chem.* **279**, 52059-52068.

Dolmetsch RE., Xu K., and Lewis RS (1998). Calcium oscillations increase the efficiency and specificity of gene expression. *Nature*. **392**, 933-936.

Drachman DA., and Sahakian BJ (1980). Memory and cognitive function in the elderly. A preliminary trial of physostigmine. *Arch. Neurol.* **37**, 674-675.

Dziegielewska KM., Saunders NR., Evans CA., Skacel PO., Haggendal CJ., Heiwall PO., and Dahalstrom AB (1976). Effects of colchicine and vinblastine on axonal transport of choline acetyltransferase in rat sciatic nerve. *Acta Physiol. Scand.* **96**, 486-494.

Eggena P., Zhu JH., Clegg K., and Barrett JD (1993). Nuclear angiotensin receptors induce transcription of renin and angiotensinogen mRNA. *Hypertension*. **22**, 496-501.

Eng LF., Uyeda CT., Chao LP., and Wolfgram F (1974). Antibody to bovine choline-acetyltransferase and immunofluorescent localization of enzyme in neurons. *Nature*. **250**, 243-245.

Erickson ES., Mooren OL., Moore D., Krogmeier JR., and Dunn RC (2006). The role of nuclear envelope calcium in modifying nuclear pore complex structure. *Can. J. Physiol. Pharmacol.* **84**, 309-318.

Feldman HH., Jacova C., Robillard A., Garcia A., Chow T., Borrie M., Schipper HM. Blair M., Kertesz A., and Chertkow H (2008). Diagnosis and treatment of dementia: 2. Diagnosis. *CMAJ.* **178**, 825-836.

Fibiger HC (1982). The organization and some projections of cholinergic neurons of the mammalian forebrain. *Brain Res.* **257**, 327-388.

Fischer A., Sananbenesi F., Schrick C., Spiess J., and Radulovic J (2002). Cyclin-dependent kinase 5 is required for associative learning. *J. Neurosci.* **22**, 3700-3707.

Folstein MF., Folstein SE., and McHugh PR (1975). Mini-Mental State: a practical method for grading the state of patients for the clinician. *J. Psychiatr. Res.* **12**, 189-198.

Fonnum F (1969). Radiochemical microassays for the determination of choline acetyltransferase and acetylcholinesterase activities. *Biochem. J.* **115**, 465-479.

Gakhar-Koppole N., Hundeshagen P., Mandl C., Weyer SW., Allinquant B., Muller U., and Ciccolini F (2008). Activity requires soluble amyloid precursor protein alpha to promote neurite outgrowth in neural stem cell-derived neurons via activation of the MAPK pathway. *Eur. J. Neurosci.* **28**, 871-872.

Games D., Adams D., Alessandrini R., Barbour R., Berthelette P., Blackwell C., Carr T., Clemens J., Donaldson T., Gillespie F., et al (1995). Alzheimer-type neuropathology in transgenic mice overexpressing V717F beta-amyloid precursor protein. *Nature.* **373**, 523-527.

Garcia-Alloza M., Robbins EM., Zhang-Nunes SX., Purcell SM., Betensky RA., Raju S., Prada C., Greenberg SM., Bacskai BJ., Frosch MP (2004) Characterization of amyloid deposition in the APPswe/PS1dE9 mouse model of Alzheimer disease. *Neurobiol. Dis.* **24**, 516-524.

Gauthier S (2002). Advances in the pharmacotherapy of Alzheimer's disease. *Can. Med. Assoc. J.* **166**, 616-623.

George CH., Rogers SA., Bertrand BM., Tunwell RE., Thomas NL., Steele DS., Cox EV., Pepper C., Hazeel CJ., Claycomb WC., and Lai FA (2007). Alternative splicing of ryanodine receptors modulates cardiomyocyte Ca2+ signaling and susceptibility to apoptosis. *Circ. Res.* **100**, 874-883.

German DC., Yazdani U., Speciale SG., Pasbakhsh P., Games D., and Liang CL (2003). Cholinergic neuropathology in a mouse model of Alzheimer's disease. *J. Comp. Neurol.* **462**, 371-381.

Gill SK., Bhattacharya M., Ferguson SS., and Rylett RJ (2003). Identification of a novel nuclear localization signal common to 69- and 82-kDa human choline acetyltransferase. *J. Biol. Chem.* **278,** 20217-20224.

Gill SK., Ishak M., Dobransky T., Haroutunian V., Davis KL., and Rylett RJ (2007). 82-kDa choline acetyltransferase is in nuclei of cholinergic neurons in human CNS and altered in aging and Alzheimer disease. *Neurobiol. Aging.* **28**, 1028-1040.

Gilman S., Koller M., Black RS., Jenkins L., Griffith SG., Fox NC., Eisner L., Kirby L., Rovira MB., Forette F., and Orgogozo JM. AN1792(QS-21)-201 Study Team (2005). Clinical effects of Abeta immunization (AN1792) in patients with AD in an interrupted trial. *Neurology* **64**, 1553–1562.

Gilmor ML., Erickson JD., Varogui H., Hersh LB., Bennett DA., Cochran EJ., Mufson EJ., and Levey AI (1999). Preservation of nucleus basalis neurons containing choline acetyltransferase and the vesicular acetylcholine transporter in the elderly with mild cognitive impairment and early Alzheimer's disease. *J. Comp. Neurol.* **411**, 693-704.

Goate A., Chartier-Harlin MC., Mullan M., Brown J., Crawford F., Fidani L., Giuffra L., Haynes A., Irving N., and James L (1991). Segregation of a missense mutation in the amyloid precursor protein gene with familial Alzheimer's disease. *Nature*. **349**, 704-706.

Goedert M., Fine A., Hunt SP., and Ullrich A (1986). Nerve growth factor messenger-RNA in peripheral and central rat tissues and in the human central nervous system-lesion effects in the rat brain and levels in Alzheimer's disease. *Brain Res.* **387**, 85-92.

Greenfield JP., Tsai J., Gouras GK., Hai B., Thinakaran G., Checler F., Sisodia SS., Greengard P., and Xu H (1999). Endoplasmic reticulum and trans-Golgi network generate distinct populations of Alzheimer beta-amyloid peptides. *Proc. Natl. Acad. Sci. USA.* **96**, 742-747.

Hahm SH., Chen L., Patel C., EricksonJ., Bonner TI., Weihi E., Schafer MK., and Eiden LE (1997). Upstream sequencing and functional characterization of the human cholinergic gene locus. *J. Mol. Neurosci.* **9**, 223-236.

Hamdane M., Sambo AV., Delobel P., Begard S., Violleau A., Delacourte A., Bertrand P., Benavides J., and Buee L (2003). Mitotic-like tau phosphorylation by p25-Cdk5 kinase complex. *J. Biol. Chem.* **278**, 34026-34034.

Han P., Dou F., Li F., Zhang X., Zhang YW., Zheng H., Lipton SA., Xu H., and Liao FF (2005). Suppression of cyclin-dependent kinase 5 activation by amyloid precursor protein: a novel excitoprotective mechanism involving modulation of tau phosphorylation. *J. Neurosci.* **25**, 11542-11552.

Haniu M., Denis P., Young Y., Mendiaz EA., Fuller J., Hui JO., Bennett BD., Kahn S., Ross S., Burgess T., Katta V., Rogers G., Vassar R., and Citron M (2000). Characterization of Alzheimer's beta -secretase protein BACE. A pepsin family member with unusual properties. *J. Biol. Chem.* **275**, 21099-21106.

Hardy J., and Selkoe DJ (2002). The amyloid hypothesis of Alzheimer's disease: progress and problems on the road to therapeutics. *Science* **297**, 353-356.

Harkany T., Varga C., Grosche J., Mulder J., Luiten PG., Hortobagyi T., Penke B., Hartig W (2002). Distinct subsets of nucleus basalis neurons exhibit similar sensitivity to excitotoxicity. *Neuroreport.* **13**, 767-772.

Heneka MT., Nadrigny F., Regen T., Martinez-Hernandez A., Dumitrescu-Ozimek L., Terwel D., Jardanhazi-Kurutz D., Walter J., Kirchhoff F., Hanisch UK., and Kummer MP (2010). Locus ceruleus controls Alzheimer's disease pathology by modulating microglial functions through norepinephrine. *Proc. Natl. Acad. Sci. USA.* **107**, 6058-6063.

Henke H., and Lang W (1983). Cholinergic enzymes in neocortex, hippocampus and basal forebrain of non-neurological and senile dementia of alzheimer-type patients. *Brain Res.* **267**, 281-291.

Hernandez CM., Kayed R., Zheng H., Sweatt JD., and Dineley KT (2010). Loss of alpha7 nicotinic receptors enhances beta-amyloid oligomer accumulation, exacerbating early-stage cognitive decline and septohippocampal pathology in a mouse model of Alzheimer's disease. *J. Neurosci.* **30**, 2442-2453.

Hernandez D., Sugaya K., Qu TY., McGowan E., Duff K., and McKinney M (2001). Survival and plasticity of basal forebrain cholinergic systems in mice transgenic for presenilin-1 and amyloid precursor protein mutant genes. *Neuroreport.* **12**, 1377-1384.

Hsiao K., Chapman P., Nilsen S., Eckman C., Harigaya Y., Younkin S., Yang F., and Cole G (1996). Correlative memory deficits, Aβ elevation, and amyloid plaques in transgenic mice. *Science.* **274**, 99-102.

Huse JT., Liu K., Pijak DS., Carlin D., Lee VM., and Doms RW (2002). Beta-secretase processing in the trans-Golgi network preferentially generates truncated amyloid species that accumulate in Alzheimer's disease brain. *J. Biol. Chem.* **277**, 16278-16284.

Huse JT., Pijak DS., Leslie GJ., Lee VM., and Doms RW (2000). Maturation and endosomal targeting of beta-site amyloid precursor protein-cleaving enzyme. The Alzheimer's disease beta-secretase. *J. Biol. Chem.* **275**, 33729-33737.

Iijima K., Ando K., Takeda S., Satoh Y., Seki T., Itohara S., Greengard P., Kirino Y., Narin AC., and Suzuki T (2000). Neuron-specific phosphorylation of Alzheimer's beta-amyloid precursor protein by cyclin-dependent kinase 5. *J. Neurochem.* **75**, 1085-1091.

Iwatsubo T (1998). Amyloid beta protein in plasma as a diagnostic marker for Alzheimer's disease. *Neurobiol. Aging* **19**, 161-163.

Jankowsky JL., Fadale DJ., Anderson J., Xu GM., Gonzales V., Jenkins NA., Copeland NG., Lee MK., Younkin LH., Wagner SL., Younkin SG., and Borchelt DR (2004). Mutant presenilins specifically elevate the levels of the 42 residue β-amyloid peptide *in vivo*: evidence for augmentation of a 42-specific γ secretase. *Hum. Mol. Genet.* **13**, 159-170.

Kar S., Fan J., Smith MJ., Goedert M., and Amos LA (2003). Repeat motifs of tau bind to the insides of microtubules in the absence of taxol. *EMBO J.* **22**, 70-77.

Kasashima S., Muroishi Y., Futakuchi H., Nakanishi I., and Oda Y (1998). In situ hybridization study of the distribution of choline acetyltransferase in the human brain. *Brain Res.* **806**, 8-15.

Kim AR., Rylett RJ., and Shilton BH (2006). Substrate binding and catalytic mechanism of human choline acetyltransferase. *Biochemistry.* **45**, 14621-14631.

Klunk WE., Engler H., Nordberg A., Wang Y., Blomqvist G., Holt DP., Bergström M., Savitcheva I., Huang GF., Estrada S., Ausén B., Debnath ML., Barletta J., Price JC., Sandell J., Lopresti BJ., Wall A., Koivisto P., Antoni G., Mathis CA., and Långström B (2004). Imaging brain amyloid in Alzheimer's disease with Pittsburgh Compound-B. *Ann. Neurol.* **55**, 306–319.

Koh JY., Yang LL., and Cotman CW (1990). Beta-amyloid protein increases the vulnerability of cultured cortical neurons to excitotoxic damage. *Brain Res.* **533**, 315–320.

Koh YH., von Arnim CA., Hyman BT., Tanzi RE., and Tesco G (2005). BACE is degraded via the lysosomal pathway. *J. Biol. Chem.* **280**, 32499-32504.

Kuhar M J., and Murrin LC (1978). Sodium-dependent, high-affinity choline uptake. *J. Neurochem.* **30,** 15–21.

Lee HC., Fellenz-Maloney MP., Liscovitch M., and Blusztajn JK (1993). Phospholipase D-catalyzed hydrolysis of phosphatidylcholine provides the choline precursor for acetylcholine synthesis in a human neuronal cell line. *Proc. Natl. Acad. Sci. USA.* **90**, 10086-10090.

Lee M., Kwon YT., Li M., Peng J., Friedlander RM., and Tsai LH (2000). Neurotoxicity induces cleavage of p35 to p25 by calpain. *Nature.* **405**, 360-364.

Lim RY., Ullman KS., and Fahrenkrog B (2008). Biology and biophysics of the nuclear pore complex and its components. *Int. Rev. Cell Mol. Biol.* **267**, 299-342.

Lind GJ., and Cavanagh HD (1993). Nuclear muscarinic acetylcholine receptors in corneal cells from rabbit. *Invest. Ophthalmol. Vis. Sci.* **34**, 2943-2952.

Lind GJ., and Cavanagh HD (1995). Identification and subcellular distribution of muscarinic acetylcholine receptor-related proteins in rabbit corneal and Chinese hamster ovary cells. *Invest. Ophthalmol. Vis. Sci.* **36**, 1492-1507.

Liu F., Su Y., Li B., Zhou Y., Ryder J., Gonzalez-DeWhitt P., May PC., and Ni B (2003). Regulation of amyloid precursor protein (APP) phosphorylation and processing by p35/Cdk5 and p25/Cdk5. *FEBS Lett.* **547**, 193-196.

Lonnerberg PL., Schoenherr CJ., Anderson DJ., and Ibanez CF (1996). Cell type-specific regulation of Choline Acetyltransferase gene expression. *J. Biol. Chem.* **271**, 33358-33365.

Machova E., Jakubik J., Michal P., Oksman M., Iivonen H., Tanila H., and Dolezal V (2008). Impairment of muscarinic transmission in transgenic APPswe/PS1dE9 mice. *Neurobiol. Aging.* **29**, 368-378.

Machova E., Rudajev V., Smyckova H., Koivisto H., Tanila H., and Dolezal V (2010). Functional cholinergic damage develops with amyloid accumulation in young adult APPswe/PS1dE9 transgenic mice. *Neurobiol. Dis.* **38**, 27-35.

Mayerhofer A., and Kunz L (2005). A non-neuronal cholinergic system of the ovarian follicle. *Ann. Anat.* **187**, 521-528.

Mazanetz MP., and Fischer PM (2007). Untangling tau hyperphosphorylation in drug design for neurodegenerative diseases. *Nat. Rev. Drug Discov.* **6**, 464-479.

Mesulam MM (1988). Central cholinergic pathways: neuroanatomy and some behavioral implications. In *Neurotransmitters and cortical function* (Avoli M., Reader TA., Dykes RW., and Gloor P. eds), pp. 237–260.

Mesulam MM (1995). Structure and function of cholinergic pathways in the cerebral cortex, limbic system, basal ganglia, and thalamus of the human brain. In *Psychopharmacology: The fourth generation of progress* (Bloom FE., and Kupfer DJ., eds), pp. 135-146.

Mesulam MM (1996). The systems-level organization of cholinergic innervation in the human cerebral cortex and its alterations in Alzheimer's disease. *Prog. Brain Res.* **109**, 285-297.

Michelsen KA., Prickaerts J., and Steinbusch HW (2008). The dorsal raphe nucleus and serotonin: implications for neuroplasticity linked to major depression and Alzheimer's disease. *Prog. Brain Res.* **172**, 233-264.

Misawa H., Matsuura J., Oda Y., Takahashi R., and Deguchi T (1997). Human choline acetyltransferase mRNAs with different 5'-region produce a 69-kDa major translation product. *Mol. Brain Res.* **44**, 323-333.

Morris JC (1993). The Clinical Dementia Rating (CDR): Current version and scoring rules. Neurology. **43**, 2412-2414.

Morris JC (1997). Clinical dementia rating: a reliable and valid diagnostic and staging measure for dementia of the Alzheimer type. *Int. Psychogeriatr.* **9 Suppl 1**, 173-176.

Mountjoy CQ., Rossor MN., Iversen LL., and Roth M (1984). Correlation of cortical cholinergic and GABA deficits with quantitative neuropathological findings in senile dementia. *Brain.* **107**, 507–518.

Nachmansohn D., and Machado AL (1943). The formation of acetylcholine. A new enzyme: choline acetylase. *J. Neurophysiol.* **6**, 397-403.

Ng P., Parks RJ., Cummings DT., Evelegh CM., Sankar U., and Graham FL (1999). A high-efficiency Cre/*loxP*-based system for construction of adenoviral vectors. *Hum. Gene Ther.* **10**, 2667-2672.

Nguyen ML., Cox GD., and Parsons SM (1998). Kinetic parameters for the vesicular acetylcholine transporter: two protons are exchanged for one acetylcholine. *Biochemistry.* **37**, 13400-13410.

Nikolaev A., McLaughlin T., O'Leary DD., and Tessier-Lavigne M (2009). APP binds DR6 to trigger axon pruning and neuron death via distinct caspases. *Nature*. **457**, 981-989.

Nikolic M., Dudek H., Kwon YT., Ramos YF., and Tsai LH (1996). The cdk5/p35 kinase is essential for neurite outgrowth during neuronal differentiation. *Genes Dev*. **10**, 816-825.

Nilsson L., Nrodberg A., Hardy J., Wester P., and Winblad B (1986). Physostigmine restores ^{3}H-acetylcholine efflux from Alzheimer brain slices to normal level. *J. Neural Transm*. **67**, 275-285.

Noguchi A., Mtsumura S., Dezawa M., Tada M., Yanazawa M., Ito A., Akioka M., Kikuchi S., Sato M., Ideno S., Noda M., Fukunari A., Muramatsu S., Itokazu Y., Sato K., Takahashi H., Teplow DB., Nabeshima Y., Kakita A., Imahori K., and Hoshi M (2009). Isolation and characterization of patient derived, toxic, high mass amyloid beta-protein (Abeta) assembly from Alzheimer disease brains. *J. Biol. Chem*. **284**, 32895-32905.

O'Connor T., Sadleir KR., Maus E., Velliquette RA., Zhao J., Cole SL., Eimer WA., Hitt B., Bembinster LA., Lammich S., Lichtenthaler SF., Hebert SS., De Strooper B., Haass C., Bennett DA., and Vassar R (2008). Phosphorylation of the translation initiation factor eIF2alpha increases BACE1 levels and promotes amyloidogenesis. *Neuron*. **60**, 988-1009.

Oda Y., Nakanishi I., and Deguchi T (1992). A complementary DNA for human choline acetyltransferase induces two forms of enzyme with different molecular weights in cultured cells. *Mol. Brain Res*. **16**, 287-294.

Oda Y (1999). Choline acetyltransferase: The structure, distribution and pathologic changes in the central nervous system. *Pathol. Int*. **49**, 921-937.

Oddo S., Caccamo A., Shepherd JD., Murphy P., Golde TE., Kayed R., Metherate R., Mattson MP., Akbari Y., and LaFerla FM (2003). Triple-Transgenic Model of Alzheimer's Disease with Plaques and Tangles: Intracellular Aβ and Synaptic Dysfunction. *Neuron*. **39**, 409-421.

Ohno K., Tsujino A., Brengman JM., Harper CM., Bajzer Z., Udd B., Beyring R., Robb S., Kirkham FJ., and Engel AG (2001). Choline acetyltransferase mutations cause myasthenic syndrome associated with episodic apnea in humans. *Proc. Natl. Acad. Sci. USA*. **98**, 2017–2022.

Okuda T., Haga T., Kanai Y., Endou H., Ishihara T., and Katsura I (2000). Identification and characterization of the high-affinity choline transporter. *Nat. Neurosci.* **3**, 120-125.

Orgogozo JM., Gilman S., Dartigues JF., Laurent B., Puel M., Kirby LC., Jouanny P., Dubois B., Eisner L., Flitman S., Michel BF., Boada M., Frank A., and Hock C (2003). Subacute meningoencephalitis in a subset of patients with AD after Abeta42 immunization. *Neurology.* **61**(1):46–54.

Pahud G., Salem N., van de Goor J., Medilanski J., Pellegrinelli N., and Deder-Colli L (1998). Study of subcellular localization of membrane-bound choline acetyltransferase in Drosophila central nervous system and its association with membranes. *Eur. J. Neurosci.* **10**, 1644-1653.

Patrick GN., Zukerberg L., Nikolic M., de la Monte S., Dikkesk P., and Tsai LH (1999). Conversion of p35 to p25 deregulates Cdk5 activity and promotes neurodegeneration. *Nature*. **402**, 615-622.

Perez SE., Dar S., Ikonomovic MD., DeKosky ST., and Mufsona EJ (2007). Cholinergic forebrain degeneration in the APPswe/PS1ΔE9 transgenic mouse. *Neurobiol. Disease*. **28**, 3-15.

Perry EK., Gibson PH., Blessed G., Perry RH., and Tomlinson BE (1977). Neurotransmitter enzyme abnormalities in senile dementia: choline-acetltransferase and glutamic-acid decarboxylase activities in necropsy brain-tissue. *J. Neurol. Sci.* **34**, 247-265.

Perry EK., Blessed G., Tomlinson BE., Perry RH., Crow TJ., Cross AJ., Dockray GJ., Dimaline R., and Arregui A (1981). Neurochemical activities in human temporal lobe related to aging and Alzheimer's type changes. *Neurobiol. Aging.* **2**, 251–256.

Price JL., and Morris JC (1999). Tangles and plaques in nondemented aging and "preclinical" Alzheimer's disease. *Ann. Neurol.* **45**, 358–368.

Qing H., Zhou W., Christensen MA., Sun X., Tong Y., and Song W (2004). Degradation of BACE by the ubiquitin-proteasome pathway. *FASEB J.* **18**, 1571-1573.

Resendes MC., Dobransky T., Ferguson SS., and Rylett RJ (1999). Nuclear localization of the 82-kDa form of human choline acetyltransferase. *J. Biol. Chem.* **274,** 19417-19421.

Richardson PJ (1986). Choline uptake and metabolism in affinity-purified cholinergic nerve terminals from rat brain. *J. Neurochem.* **46,** 1251-1255.

Riemenschneider M., Lautenschlager N., Wagenpfeil S., Diehl J., Drzezga A., and Kurz A (2002). Cerebrospinal fluid tau and beta-amyloid 42 proteins identify Alzheimer disease in subjects with mild cognitive impairment. *Arch. Neurol.* **59**, 1729–1734.

Ritchie CW., Ames D., Clayton T., and Lai R (2004). Meta-analysis of randomized trials of the efficacy and safety of donepezil, galantamine, and rivastigmine for the treatment of Alzheimer's disease. *Am. J. Geriatr. Psychiatry.* **12**, 358-369.

Robner S., Ueberham U., Schliebs R., Perez-Polo JR., and Bigl V (1998). The regulation of amyloid precursor protein metabolism by cholinergic mechanisms and neurotrophin receptor signalling. *Prog. Neurobiol.* **56**, 541-569.

Rockwood K (2004). Size of the treatment effect on cognition of cholinesterase inhibition in Alzheimer's disease. *J. Neurl. Neurosurg. Psychiatry.* **75**, 677-685.
Rogaev EI., Sherrington R., Rogaeva EA., Levesque G., Ikeda M., Liang Y., Chi H., Lia C., Holman K., Tsuda T., Mar L., Sorbi S., and Nacmlas B (1995). Familial Alzheimer's disease in kindreds with missense mutations in a gene on chromosome 1 related to the Alzheimer's isease type 3 gene. *Nature.* **376**, 775-778.

Rogers SL., Doody RS., Mohs RC., and Friedhoff LT (1998). Donepezil improves cognition and global function in Alzheimer disease: a 15-week, double-blind, placebo-controlled study. Donepezil Study Group. *Arch. Intern. Med.* **158**, 1021-1031.

Rowe CC., Ng S., Ackermann U., Gong SJ., Pike K., Savage G., Cowie TF., Dickinson KL., Maruff P., Darby D., Smith C., Woodward M., Merory J., Tochon-Danguy H., O'Keefe G., Klunk WE., Mathis CA., Price JC., Masters CL., and Villemagne VL (2007). Imaging beta-amyloid burden in aging and dementia. *Neurology* **68**, 1718–1725.

Rumble B., Retallack R., Hilbich C., Simms G., Multhaup G., Martins R., Hockey A., Montgomery P., Bevreuther K., and Masters CL (1989). Amyloid A4 protein and its precursor in Down's syndrome and Alzheimer's disease. *N. Engl. J. Med.* **320**, 1446-1452.

Rylett RJ., Ball MJ., and Colhoun EH. (1983). Evidence for high affinity choline transport in synaptosomes prepared from hippocampus and neocortex of patients with Alzheimer's disease. *Brain Res.* **289**, 169-175.

Savonenko A., Xu GM., Melnikova T., Morton JL., Gonzales V., Wong MPF., Price DL., Tang F., Markowska AL., and Borchelta DR (2005). Episodic-like memory deficits in the APPswe/PS1dE9 mouse model of Alzheimer's disease: Relationships to β-amyloid deposition and neurotransmitter abnormalities. *Neurobiol Disease.* **18**, 602-617.

Schenk D., Barbour R., Dunn W., Gordon G., Grajeda H., Guido T., Hu K., Huang J., Johnson-Wood K., Khan K., Kholodenko D., Lee M., Liao Z., Lieberburg I., Motter R., Mutter L., Soriano F., Shopp G., Vasquez N., Vandevert C., Walker S., Wogulis M., Yednock T., Games D., and Seubert P (1999). Immunization with amyloid-beta attenuates Alzheimer-disease-like pathology in the PDAPP mouse. *Nature* **400,** 173–177.

Schindowski K., Belarbi K., and Buee L (2008). Neurotrophic factors in Alzheimer's disease: role of axonal transport. *Genes Brain Behav.* **7** (Suppl 1), 43-56.

Schmidt BM., and Rylett RJ (1993). Phosphorylation of rat brain choline acetyltransferase and its relationship to enzyme activity. *J. Neurochem.* **61**, 1774-1781.

Schraufstatter IU., Discipio RG., and Khaldoyanidi SK (2010). Alpha 7 subunit of nAChR regulates migration of human mesenchymal stem cells. *J. Stem Cells.* **4**, 203-216.

Seshadri S., Drachman DA., and Lippa CF (1995). Apolipoprotein E epsilon 4 allele and the lifetime risk of Alzheimer's disease: what physicians know, and what they should know. *Arch. Neurol.* **52,** 1074-1079.

Sisodia SS (1992). Beta-amyloid precursor protein cleavage by a membrane-bound protease. *Proc. Natl. Acad. USA.* **89**, 6075-6079.

Sucher NJ., Lipton SA., and Dreyer EB (1997). Molecular basis of glutamate toxicity in retinal ganglion cells. *Vision Res.* **37**, 3483–3493.

Sunderland T., Linker G., Mirza N, Putnam KT., Friedman DL., Kimmel LH., Bergeson J., Manetti GJ., Zimmerman M., Tang B., Bartko JJ., and Cohen RM (2003). Decreased beta-amyloid1–42 and increased tau levels in cerebrospinal fluid of patients with Alzheimer disease. *JAMA.* **289**, 2094-2103.

Suzuki T. And Nakaya T (2008). Regulation of amyloid β-protein precursor by phosphorylation and protein interactions. *J. Biol. Chem.* **283**, 29633-29637.

Tan TC., Valova VA., Malladi CS., Graham ME., Berven LA., Jupp OJ., Hansra G., McClure SJ., Sarcevic B., Boadle RA., Larsen MR., Cousin MA., and Robinson PJ (2003). Cdk5 is essential for synaptic vesicle endocytosis. *Nat. Cell Biol.* **5**, 701-710.

Tariot PN., Farlow MR., Grossberg GT, Graham SM., McDonald S., and Gergel I (2004). Memantine treatment in patients with moderate to severe Alzheimer's disease already receiving donepezil: a randomized controlled trial. *JAMA.* **291**, 317–324.

Thakur A., Siedlak SL., James SL., Bonda DJ., Rao A., Webber KM., Camins A., Pallas M., Casadesus G., Lee H., Bowser R., Raina AK., Perry G., Smith MA., and Zhu X (2008). Retinoblastoma protein phosphorylation at multiple sites is associated with neurofibrillary pathology in Alzheimer disease. *Int. J. Clin. Exp. Pathol.* **1**, 134-146.

Thinakaran G., and Koo EH. (2008) Amyloid precursor protein trafficking, processing, and function. *J. Biol. Chem.* **283**, 29615-29619.

Thornton E., Vink R., Blumbergs PC., and Van Den Heuvel C (2006). Soluble amyloid precursor protein alpha reduces neuronal injury and improves functional outcome following diffuse traumatic brain injury in rats. *Brain Res.* **1094**, 38-46.

Tiraboschi P., Hansen LA., Alford M., Masliah E., Thal LJ., and Correy-Bloom J (2000). The decline in synapses and cholinergic activity is asynchronous in Alzheimer's disease. *Neurology* **55**, 1278–1283.

Town T., Zolton J., Shaffner R., Schnell B., Crescentini R., Wu Y., Zeng J., DelleDonne A., Obregon D., Tan J., and Mullan M (2002). p35/Cdk5 pathway mediates soluble amyloid-β peptide-induced tau phosphorylation *in vitro*. *J. Neurosci. Res.* **69**, 362-372.

Vale C., Alonso E., Rubiolo JA., Vieytes MR., LaFerla FM., Gimenez-Llort L., and Botana LM (2010). Profile for amyloid-β and tau expression in primary cortical cultures from 3xTg-AD mice. *Cell Mol. Neurobiol.* **30**, 577-590.

Vanmechelen E., Vanderstichele H., Davidsson P., Van Kerschaver E., Van Der Perre B., Sjogren M., Andreasen N., and Blennow K (2000). Quantification of tau phosphorylated at threonine 181 in human cerebrospinal fluid: a sandwich ELISA with a synthetic phosphopeptide for standardization. *Neurosci. Lett.* **285**, 49–52.

Varvel NH., Bhaskar K., Patil AR., Pimplikar SW., Herrup K., and Lamb BT (2008). Aβ oligomers induce neuronal cell cycle events in Alzheimer's disease. *J. Neurosci.* **28**, 10786-10793.

Vassar R., Bennett BD., Babu-Khan S., Khan S., Mendiaz EA., Denis P., Teplow DB., Ross S., Amarante P., Loeloff R., Luo Y., Fisher S., Fuller J., Edenson S., Lile J., Jarosinski MA., Biere AL., Curran E., Burgess T., Louis JC., Collins F., Treanor J., Rogers G., and Citron M (1999). β-secretase cleavage of Alzheimer's amyloid precursor protein by the transmembrane aspartic protease BACE. *Science.* **286**, 735-741.

Vassar R (2004). BACE1: the beta-secretase enzyme in Alzheimer's disease. *J. Mol. Neurosci.* **23**,105-114.

Von Rotz RC., Kohli BM., Bosset J., Meier M., Suzuki T., Nitsch RM., and Konietzko U (2004). The APP intracellular domain forms nuclear multiprotein complexes and regulates the transcription of its own precursor. *J. Cell Sci.* **117**, 4435-4448.

Walter J., Fluhrer R., Hartung B., Willem M., Kaether C., Capell A., Lammich S., Multhaup G., and Haass C (2001). Phosphorylation regulates intracellular trafficking of beta-secretase. *J. Biol. Chem.* **276**, 14634-14641.

Wen Y., Yu WH., Maloney B., Bailey J., Ma J., Marie I., Maurin T., Lili W., Figueroa H., Herman M., Krishnamurthy P., Liu L., Planel E., Lau L., Lahiri DK., and Duff K (2008). Transcriptional regulation of β-secretase by p25/cdk5 leads to enhanced amyloidogenic processing. *Neuron.* **57,** 680-690.

Whitehouse PJ., Price DL., Clark AW., Coyle JT., and DeLong MR (1981). Alzheimer disease: evidence for selective loss of cholinergic neurons in the nucleus basalis. *Ann. Neurol.* **10**, 122–126.

Wooten GF., and Cheng CH (1980). Transport and turnover of acetylcholinesterase and choline acetyltransferase in rat sciatic nerve and skeletal muscle. *J. Neurochem.* **34,** 359-366.

Winblad B., and Poritis N (1999). Memantine in severe dementia: results of the 9M-Best Study (Benefit and efficacy in severely demented patients during treatment with memantine). *Intr. J. Geriatr. Psych.* **14**, 135–146.

Xu H., Sweeney D., Wang R., Thinakaran G., Lo AC., Sisodia SS., Greengard P., and Gandy S (1997). Generation of Alzheimer beta-amyloid protein in the trans-Golgi network in the apparent absence of vesicle formation. *Proc. Natl. Acad. Sci. USA.* **94**, 3748-3752.

Yang Y., Geldmacher DS., and Herrup K (2001). DNA replication precedes neuronal cell death in Alzheimer's disease. *J. Neurosci.* **21**, 2661-2668.

Yang Y., Varvel NH., Lamb BT., and Herrup K (2006). Ectopic cell cycle events link human Alzheimer's disease and amyloid precursor protein transgenic mouse models. *J. Neurosci.* **26**, 775-784.

Zambrzycka A., Alberghina M., and Strosznajder JB (2002). Effects of aging and amyloid-β peptides on choline acetyltransferase activity in rat brain. *Neurochem. Res.* **27**, 277-281.

Zarow C., Lyness SA., Mortimer JA., and Chui HC (2003). Neuronal loss is greater in the locus coeruleus than nucleus basalis and substantia nigra in Alzheimer and Parkinson diseases. *Arch. Neurol.* **60**, 337–334.

Zhang S., Salemi J., Hou H., Zhu Y., Mori T., Giunta B., Obregon D., and Tan J (2010). Rapamycin promotes β-amyloid production via ADAM-10 inhibition. *Biochem. Bioph. Res. Co.* **398**, 337-341.

APPENDIX A

Ethics approval for animal use

Western

March 11, 2010

"This is the Original Approval for this protocol"
"A Full Protocol submission will be required in 2014"

Dear Dr. Rylett:

Your Animal Use Protocol form entitled:
Modulation of Neuronal Gene Expression by Choline Acetyltransferase
Funding Agency Alzheimer's Association - Grant #R1588A15 [speedcode RRYT] - agency grant number IIRG-08-91279.

has been approved by the University Council on Animal Care. This approval is valid from **March 11, 2010** to **March 31,. 2011.** The protocol number for this project is **2010-025.**

1. This number must be indicated when ordering animals for this project.
2. Animals for other projects may not be ordered under this number.
3. If no number appears please contact this office when grant approval is received.
   If the application for funding is not successful and you wish to proceed with the project, request that an internal scientific peer review be performed by the Animal Use Subcommittee office.
4. Purchases of animals other than through this system must be cleared through the ACVS office. Health certificates will be required.

ANIMALS APPROVED FOR 4 Years

Species	4 Year Total Numbers Estimated as Required	List All Strain(s)	Age / Weight
Mouse	Group A - 20 mice	Group A - B6.Cg-Tg (APPswe,PSEN1dE9)85Dbo/J	3 - 12 months
	Group B - 240 mice	Group B - wild type female Black 6 mice	2 - 3 months

REQUIREMENTS/COMMENTS
Please ensure that individual(s) performing procedures on live animals, as described in this protocol, are familiar with the contents of this document.
The holder of this Animal Use Protocol is responsible to ensure that all associated safety components (biosafety, radiation safety, general laboratory safety) comply with institutional safety standards and have received all necessary approvals. Please consult directly with your institutional safety officers.

c.c. Approval - J. Rylett, W. Lagerwerf

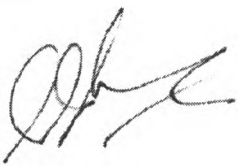

The **University *of* Western Ontario**
Animal Use Subcommittee / University Council on Animal Care
Health Sciences Centre, • London, Ontario • CANADA – N6A 5C1
PH: 519-661-2111 ext. 86770 • FL 519-661-2028 • www.uwo.ca / animal